A Comparison of Southern Hemisphere Circulation Statistics Based on GFDL and Australian Analyses

DAVID J. KAROLY*

*National Center for Atmospheric Research,** Boulder, CO 80307*

ABRAHAM H. OORT

Geophysical Fluid Dynamics Laboratory/NOAA, Princeton University, Princeton, NJ 08542

(Manuscript received 19 September 1986, in final form 20 February 1987)

ABSTRACT

Two sets of observed atmospheric circulation statistics for the Southern Hemisphere (SH) are compared. The first set was compiled at the Geophysical Fluid Dynamics Laboratory (GFDL) and consists of global objective analyses of circulation statistics accumulated at individual rawinsonde stations for the period May 1963–April 1973. The second set was obtained from daily hemispheric numerical analyses prepared operationally at the World Meteorological Centre, Melbourne, Australia for the period September 1972–August 1982. This study extends the earlier comparison of circulation statistics from station-based and from numerical analysis-based methods by Lau and Oort for the Northern Hemisphere to the Southern Hemisphere.

The domain used for the comparison is a 5° × 5° latitude–longitude grid from 10° to 90°S and seven pressure levels from 1000 to 100 mb. The circulation statistics examined include (i) ten-year averages of the monthly mean fields (measures of the mean circulation), (ii) ten-year averages of the standard deviations and covariances of daily values (measures of the daily transient eddy variability) and (iii) year-to-year standard deviations of the monthly mean fields (measures of the interannual variability). The statistics are presented using horizontal maps on pressure surfaces and latitude–pressure sections of zonal averages.

The two sets of circulation statistics were derived using very different analysis methods and they apply for different time periods. The similarities and differences between the statistics from the two datasets indicate the reliability of the statistics and can be used to define a better composite set of circulation statistics for the SH.

The relatively large differences in the statistics can generally be attributed to the sparse conventional observation network in the SH, particularly over the large ocean regions, and deficiencies in the analysis methods. The two sets agree reasonably well from 850 to 500 mb over the land masses, where the observation network is less sparse. In the upper troposphere, the magnitudes of the daily transient eddy statistics from the Australian dataset are smaller due to the analysis method and the inclusion of satellite data. Over the data-sparse regions, the use of the zonal average as the first guess for the GFDL dataset has led to reduced spatial variability, smoother fields and underestimation of extreme values.

1. Introduction

Observed atmospheric circulation statistics for the Northern Hemisphere (NH) derived from surface and upper air data and from numerical analyses have been available for a number of years (for example, Oort and Rasmusson, 1971; Newell et al., 1972, 1974; Lau et al., 1981). In the Southern Hemisphere (SH), however, the conventional surface and upper-air network is sparse and fewer studies have attempted to derive observed circulation statistics for the Southern Hemisphere. An extensive study of the mean SH circulation, described by Taljaard et al. (1969) and van Loon et al. (1971), was based on a long period of surface observations, rawinsonde observations mainly for the period 1957–66 and a build-up technique to derive upper-air fields from surface data.

Recently, two independent sets of circulation statistics for the SH have been prepared using very different methods. The first of these is based on global objective analyses of circulation statistics compiled at individual rawinsonde stations for a ten-year period, prepared at the Geophysical Fluid Dynamics Laboratory (hereafter referred to as the GFDL dataset), and is described by Oort (1983). The second set, which we shall call the Australian SH dataset (hereafter referred to as the ASH dataset), is based on ten years of daily operational numerical analyses for the SH prepared at the Australian Bureau of Meteorology. An atlas describing this dataset has been compiled (Karoly et al., 1986) and the mean circulation from the ASH dataset has been compared with the Taljaard climatology (Le Marshall et al., 1985; Karoly, 1985). Both datasets include statistics on the

* Present affiliation: Department of Mathematics, Monash University, Clayton, Vic. 3168, Australia.

** The National Center for Atmospheric Research is sponsored by the National Science Foundation.

mean circulation as well as on its daily and interannual variability.

Lau and Oort (1981, 1982) have performed an extensive comparison of observed NH circulation statistics from GFDL station-based analyses and from NMC operational daily numerical analyses for the 1963–73 period. They found that differences between the two datasets were small over the North American and Eurasian continents, but were larger over the oceans and areas of sparse data coverage. Details of a number of earlier studies of the NH circulation based on circulation statistics derived using one of the two different analysis methods were presented. More recently, Rosen et al. (1985) have compared circulation statistics for the NH derived from FGGE level III-b and station-based analyses for January and June 1979. Their study also found the largest differences over areas of sparse data coverage.

In this study, the comparison of NH circulation statistics from station-based and from numerical analysis-based methods by Lau and Oort (1981, 1982) is extended to the SH, using the GFDL and ASH datasets. We have followed the format of Lau and Oort (1981, 1982) so that the SH statistics can be compared with those from the NH. Given the sparse rawinsonde station network in the SH, this extensive comparison of the two datasets also is intended to clarify the reliability and usefulness of each set.

A limited comparison of the mean SH circulation in the GFDL dataset with some Australian analyses was described by Oort (1983). This indicated that the GFDL analyses severely underestimate the strength of the mean zonal wind in the SH. Trenberth (1982) has noted this, and also that some daily transient eddy statistics from the GFDL analyses are similar in magnitude but different in detail from those computed using eight years of Australian analyses.

In a series of papers, Trenberth has made extensive use of the operational daily analyses from the Australian Bureau of Meteorology (for a shorter period than available for the ASH dataset) as the basis for a number of studies of the SH mean circulation and transient eddies and their variability (Trenberth, 1979, 1981, 1982, 1984; Swanson and Trenberth, 1981a,b). Some of the deficiencies in the Australian analyses have been described in these studies by Trenberth and by van Loon (1980), as well as in the description of the ASH dataset (Le Marshall et al., 1985; Karoly, 1985).

Besides the detailed intercomparison of the two datasets, a brief descriptive comparison of the SH circulation statistics with those derived from FGGE analyses is given. Lau (1984) has made use of two sets of FGGE level III-b analyses prepared at GFDL and ECMWF to compare a range of circulation statistics for the whole globe derived from two different numerical analysis systems for January, February, May and June 1979. This provides a detailed comparison of circulation statistics for the SH for these months. Essentially, the same set of extensive observations, greatly expanded from the conventional synoptic network, was available for the two analysis systems and the differences between the circulation statistics are mainly due to differences in the analysis systems. These FGGE statistics provide the best estimate of the real circulation over the whole SH, allowing for their sampling of one year only. In the study described here, the differences between the two sets of circulation statistics are due to the very different methods of obtaining the statistics (station-based versus numerical analysis-based) as well as the different time periods used for the two datasets.

The intercomparison of the circulation statistics for the SH from these two datasets more clearly defines the limitations of each set. Thus, it is possible to suggest a better composite set of SH circulation statistics for studies of the general circulation of the SH and for the verification of numerical weather prediction and general circulation models.

In this paper, circulation statistics for the zonal and meridional wind components, geopotential height and temperature are compared. In a subsequent paper, a similar comparison of the circulation statistics for the water vapor field will be presented.

The two datasets are described in the next section. In section 3, the mean circulations are compared using horizontal maps of the mean fields at selected pressure levels and latitude–pressure distributions of the zonally averaged mean fields and standing eddy statistics. The daily transient eddy statistics are presented in section 4 and the interannual variability statistics are discussed in section 5 using similar diagrams. Conclusions on the reality and causes of the differences between the two datasets and on the advantages and disadvantages of each dataset are presented in section 6.

2. Description of the two datasets

The data used for this comparison consist of monthly mean fields, daily transient eddy statistics and interannual variability statistics for the zonal and meridional wind components, geopotential height and temperature for the SH winter (June, July, August) and summer (December, January, February) seasons. The data used were on a horizontal grid with five-degree resolution in latitude and longitude between 10° and 90°S and at 7 pressure levels (1000, 850, 700, 500, 300, 200 and 100 mb).

The monthly mean fields were obtained by averaging daily values over a month. The long-term average was obtained by averaging the monthly mean fields for the same calendar month over ten years. The daily transient eddy statistics were computed using daily departures from each individual monthly mean, giving daily standard deviation and covariance statistics for each month. The long-term averages of these statistics over the ten years were then computed for each calendar month. The interannual variability statistics were

computed using the monthly departures from the long-term average for each calendar month, giving monthly standard deviations. Hence, the transient eddy statistics represent the effect of the daily departures within a given month from the monthly mean for that month, whereas the interannual variability statistics represent the effect of the monthly departures from the long-term average for that calendar month. The statistics for winter and summer were taken as the average of the monthly statistics for the three winter or three summer months.

The two datasets used for the comparison are the following:

(i) *The GFDL dataset*

This set is composed of objective global analyses of monthly circulation statistics accumulated at rawinsonde stations, available from the GFDL Atmospheric Circulation Tape Library, 1958–73 (Oort, 1983). Each statistical parameter is accumulated at all individual reporting stations for the analysis period May 1963–April 1973.

A global analysis is prepared using an objective analysis method, with an initial-guess field for each parameter obtained using the zonal average of all the available data for the parameter within a 10° latitude band. Further details of the data handling procedures for the GFDL dataset have been presented in Oort (1983). A diagrammatic representation of the analysis procedure used for the GFDL dataset is shown in Fig. 1.

The GFDL dataset is available over the whole globe at a meridional resolution of 2½° latitude, but data from 10°S to 90°S at 5° latitude resolution were used for this study to ensure compatability between the two datasets. Also, data from the GFDL set were available at additional pressure levels of 950, 900, 400 and 50 mb, but were not used.

(ii) *The Australian SH dataset*

This set is based on operational daily 0000 UTC numerical analyses for the SH prepared by the World Meteorological Centre, Melbourne at the Australian Bureau of Meteorology. Details of the analysis scheme and the data handling procedure for the circulation statistics are given in Le Marshall et al. (1985) and only a brief outline of the analysis procedure is given here (shown on the right-hand side of Fig. 1).

The database for the analyses included the full conventional network, satellite imagery, satellite-derived winds and temperature soundings and drifting buoy data. Manual methods were used to specify mean sea level pressure and 1000–500 mb thickness from satellite cloud imagery where no other data were available. First, manual analyses were prepared for the mean sea level pressure and 1000–500 mb thickness over the SH. These were used to provide first-guess fields for the analysis of temperature and geopotential height. The first-guess wind fields were obtained from the analyzed height fields assuming gradient wind balance poleward of 20°S and from the climatological wind fields of Taljaard et al. (1969) at low latitudes. The numerical model 12-hour forecast fields had very little impact on the first-guess fields of wind, temperature and height for the 0000 UTC analyses because they were given low weight relative to the first-guess derived from the manual analyses. The forecast fields had greater impact on the first-guess fields for the 1200 UTC analyses, which were not used in the ASH dataset. All observations were inserted into these first-guess fields using a successive correction method as the objective analysis scheme (Cressman, 1959).

These daily numerical analyses were made on a 47 × 47 polar stereographic grid centered on the South Pole, with an effective resolution of about 500 km for the seven pressure levels given above. The circulation statistics were obtained by processing these daily gridded analyses in essentially the same way as the statistics were accumulated at individual observation sites for the GFDL dataset. However, the period used for the Australian SH dataset is from September 1972 through August 1982. The circulation statistics were then interpolated onto a 5° × 5° latitude–longitude grid from 10° to 90°S.

There is one computation-related difference between the two datasets, namely, for the standard deviations of the daily departures. In the GFDL dataset, the variance of the daily departures was calculated for each month and these variances were then averaged to provide the long-term mean. The standard deviation was estimated by taking the square root of this long-term average variance. In the ASH dataset, the square root of the variance (i.e., the standard deviation) of the daily departures was calculated separately for each month and averaged directly to obtain the long-term average standard deviation. As expected, the GFDL method gives a systematically larger value than the ASH method, with the magnitude of the increase depending on the interannual variability of the daily variance. The magnitude of this systematic increase was estimated by recomputing the long-term average standard deviation for July from the Australian daily analyses using the GFDL method. This indicated that the GFDL method leads to a small increase of about 2% only in the long-term average standard deviation, which is insignificant compared to the other differences in the statistics.

Besides the differences between the analysis methods and the periods for the analyses, there are also some differences between the conventional radiosonde network used or available for the two datasets. This is due to the different time periods and to the operational constraints on the Australian analyses. The differences are illustrated in Fig. 2, which shows the distribution of reporting rawinsonde stations for January and the number of months when reports were available for the

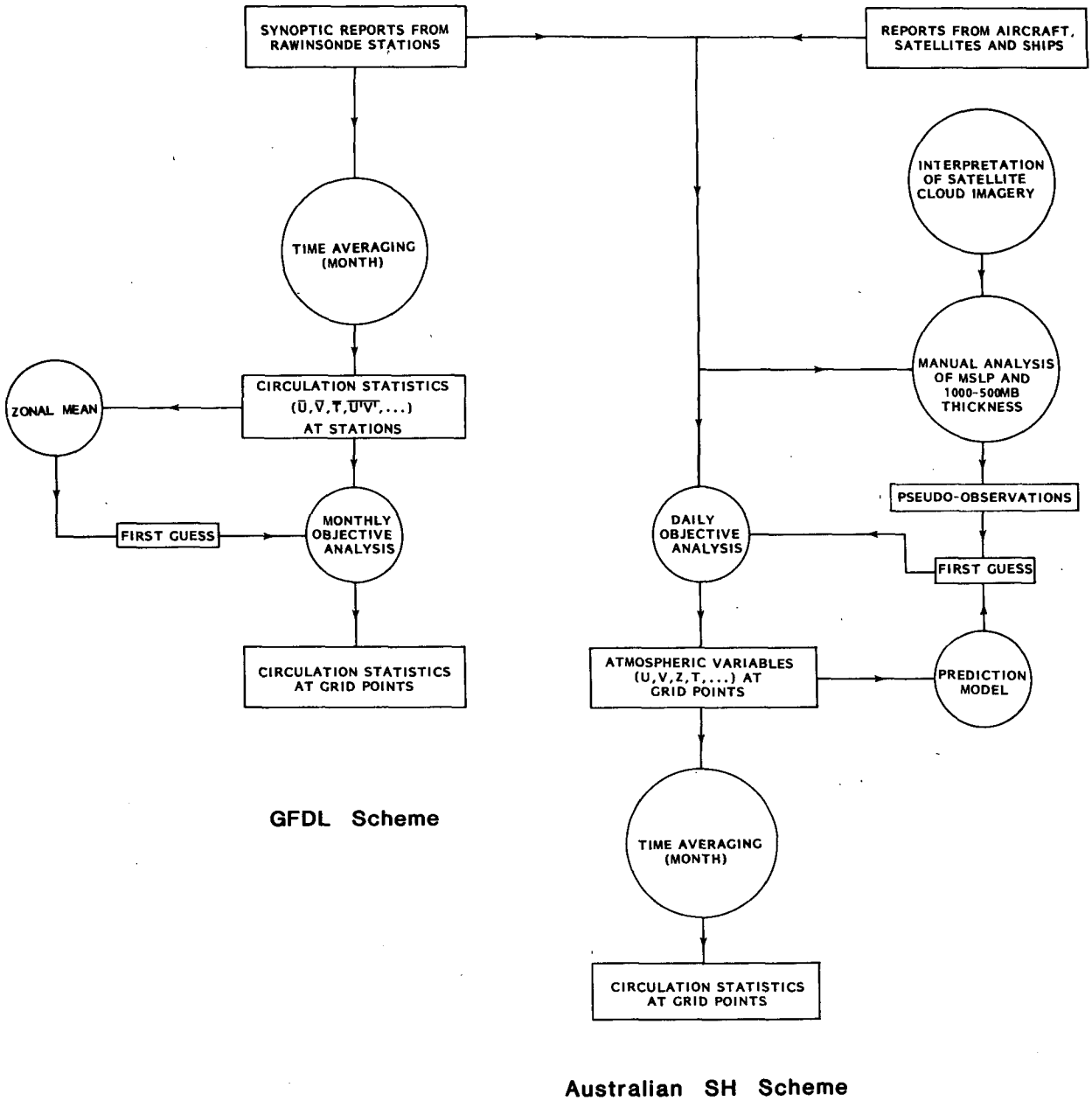

FIG. 1. Flow diagram illustrating the two different processing schemes used for compiling the circulation statistics.

two datasets. Marked at each station is the number of months out of the ten possible for which daily observations of 500 mb geopotential height were available for at least 10 days during the month. In general, the GFDL dataset has better coverage over South America due to the use of 1200 UTC data as well as 0000 UTC data versus only 0000 UTC daily analyses in the ASH dataset. Elsewhere, the coverage is better in the ASH dataset. The figures clearly show the large ocean areas in the SH with little or no conventional observation stations.

The accuracy and reliability of the GFDL and ASH datasets were further checked using monthly mean data from "Monthly Climatic Data for the World" for 20 rawinsonde stations for the 20-year period 1960–79. These WMO stations are listed in Table 1. They were chosen to give the most uniform distribution over the SH. The monthly mean data were used to give the long-term average and the interannual variability for the 20-year period at these stations. The comparison of these statistics with those from the two datasets at the station locations gives a measure of the reliability

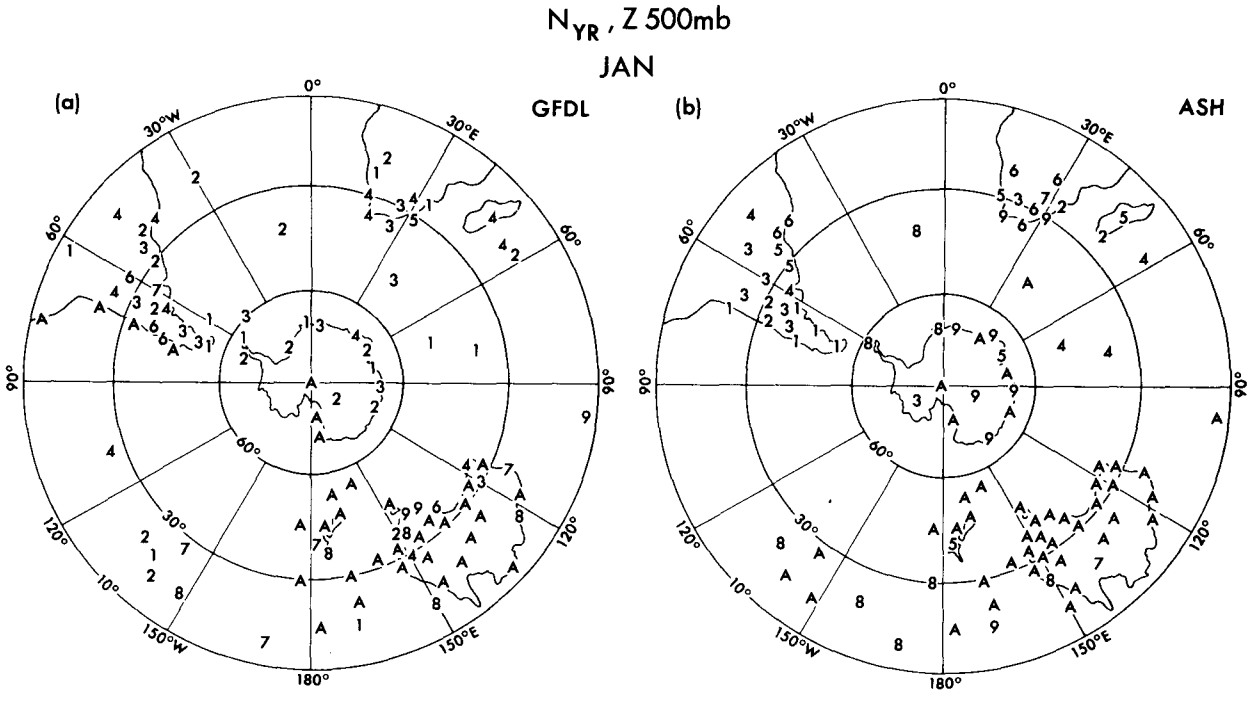

FIG. 2. Distribution of rawinsonde stations providing 500 mb geopotential height observations in January for (a) GFDL dataset and (b) Australian SH dataset. Marked at the station location is the number of January's out of the ten possible for which daily observations from the station were available for at least 10 days in the month and which were included in the analyses for each dataset. (1, 2, 3, · · ·, 8, 9, *A* = 10)

of some of the circulation statistics at the station locations. The differences of the long-term average winter values for the station data between the second ten-year period (1970–79) and the first ten-year period (1960–69) are given in Fig. 3, together with the number of winter months with station data available in each ten-year period. These differences give a measure of the real changes of the mean SH circulation between the periods.

TABLE 1. Rawinsonde stations from "Monthly Climatic Data for the World" used for checking the GFDL and ASH analyses.

WMO station	Station name	Latitude (°S)	Longitude
61996	New Amsterdam Is.	38	78°E
67774	Salisbury, Rhodesia	18	31°E
68588	Durban, South Africa	30	31°E
68816	Cape Town, South Africa	34	19°E
68906	Gough Is.	40	10°W
68994	Marion Is.	47	38°E
85442	Antofagasta, Chile	24	70°W
85799	Puerto Montt, Chile	42	73°W
87576	Ezeiza, Argentina	35	59°W
88952	Argentine Is.	65	61°W
89664	McMurdo	78	167°E
91680	Nandi, Fiji	18	178°E
91938	Tahiti	18	150°W
93119	Auckland, New Zealand	37	175°E
94120	Darwin, Australia	12	131°E
94578	Brisbane, Australia	27	153°E
94610	Perth, Australia	32	116°E
94986	Mawson	68	63°E
94998	Macquarie Is.	55	159°E
96996	Cocos Is.	12	97°E

3. Time-mean fields

a. Hemispheric distributions

Figure 4 shows the distribution of the long-term average winter mean zonal wind component at 200 mb, as given by the (a) GFDL and (b) ASH analyses. The differences between these two fields are displayed in Fig. 4c. Over almost all the SH, the zonal wind is larger in the ASH analyses, with much stronger, narrower jet streams. The largest differences occur in the jet streams over the Pacific and Indian Oceans, and exceed 10 m s^{-1}. The jet streams in the GFDL analyses appear as three discrete jets extending out from over the three SH continents, whereas in the ASH analyses there is a dominant subtropical jet extending from the Indian Ocean over Australia to the central Pacific Ocean and a polar jet south of New Zealand. The GFDL field appears to be severely smoothed compared with the ASH field over the oceans.

The GFDL and ASH values for the zonal wind at the locations of the 20 WMO rawinsonde stations were obtained from the data grids by linear interpolation.

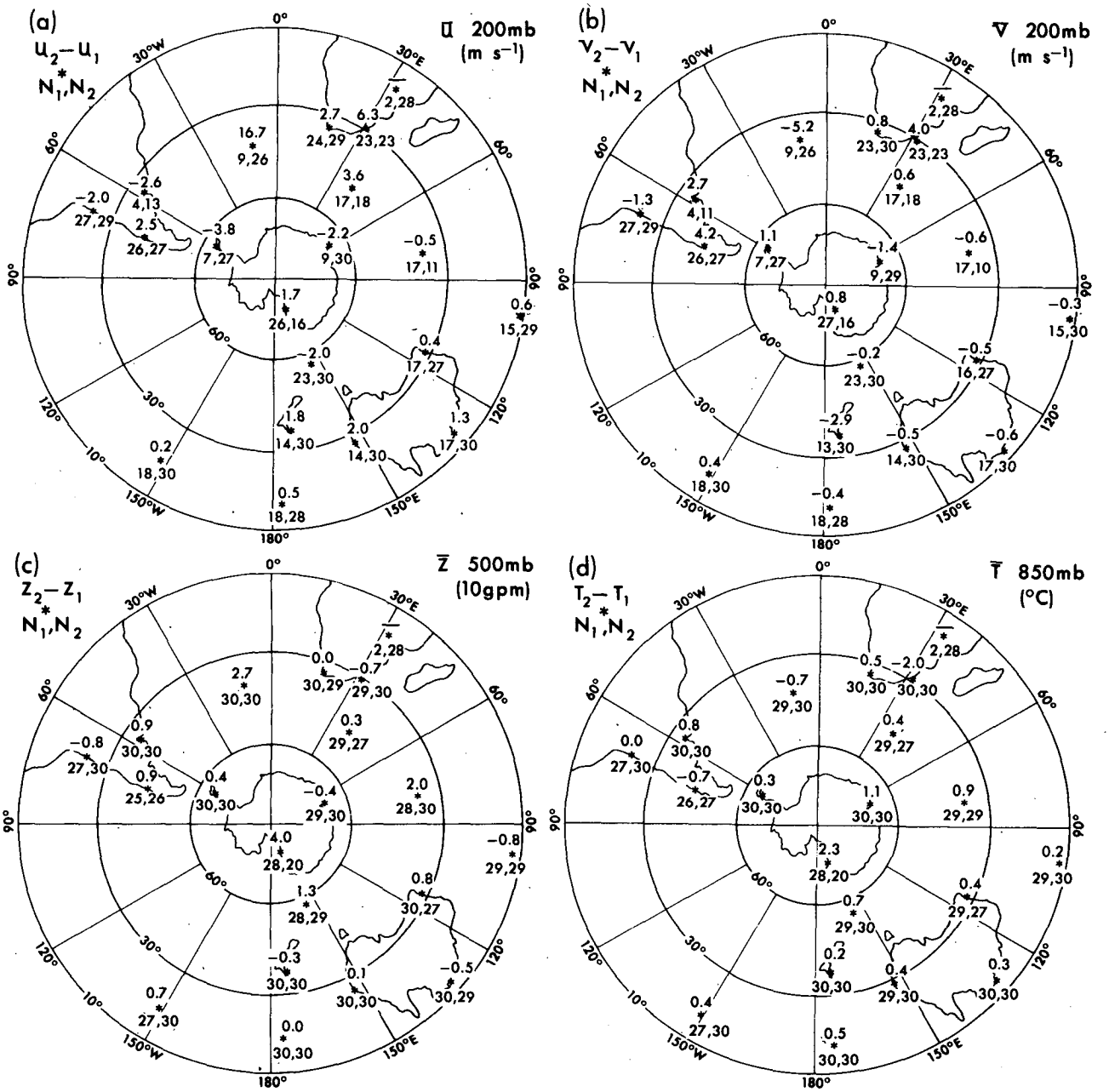

FIG. 3. Data availability and differences of the station means between the two ten-year periods for the selected rawinsonde stations used for checking the circulation statistics for (a) zonal wind at 200 mb, (b) meridional wind at 200 mb, (c) geopotential height at 500 mb and (d) temperature at 850 mb. Shown above each station location is the difference of the ten-year mean winter (JJA) station value for the second ten-year period (1970–79) minus the first (1960–69). Below each station is plotted the number of winter months (maximum 30) with monthly mean data available in the first ten-year period, on the left, and in the second, on the right.

These values were compared with the twenty-year mean values for the rawinsonde stations. In Fig. 4d, the differences between the WMO station means and the GFDL (ASH) analyses are displayed above (below) the locations of the individual stations. The differences among the three datasets are relatively small (<4 m s^{-1}) at most of the stations, with the GFDL analyses showing generally smaller and the ASH analyses larger values than the station means. The largest differences from the station means occur at stations which provided limited or no observations for the analyses, e.g. Marion Island (47°S, 38°E) for the GFDL analyses and New Amsterdam Island (38°S, 78°E) for the ASH analyses. The differences at the stations are generally

of the same order as the differences of the ten-year means of the station data between the first and second ten-year periods, shown in Fig. 3a. Therefore, the two sets fit the station data well at the station locations. Away from the station locations, over the data sparse regions, the differences between the two datasets are large. The mean zonal wind from the ASH compares better with the FGGE analyses described by Lau (1984) and the earlier SH climatology (van Loon et al., 1971).

The differences between the GFDL and ASH zonal wind data at other levels (not shown) display features which are qualitatively similar to those shown in Fig. 4c but are typically smaller in magnitude. This can be seen in the zonal average of the zonal wind to be shown later.

The GFDL and ASH analyses for the long-term average meridional wind at 200 mb and the corresponding difference map are shown in Figs. 5a–c. There is reasonable agreement between the fields over the continents (differences < 2 m s^{-1}), but over the oceans there is little agreement. The GFDL pattern is almost zonally symmetric, with a poleward wind component at low latitudes and an equatorward component in middle latitudes; the ASH pattern exhibits large zonal variations, dominated by zonal wavenumbers one and three at middle and high latitudes. The differences from the WMO station means in Fig. 5d are generally small (<2 m s^{-1}) but of the same order as the differences of the station means between the two ten-year periods in Fig. 3b, and similar in magnitude to the meridional wind itself. In the data-sparse regions, the use of the zonal-average as the first guess in the GFDL analyses has led to more zonally symmetric fields than in the ASH analyses.

The distributions of the long-term mean geopotential height at 500 mb based on the GFDL and ASH analyses and the corresponding differences are shown in Fig. 6. There is good agreement between the two datasets over the continents (differences < 20 gpm) but, over the oceans, there are much larger differences (up to 100 gpm). Again, the GFDL analyses are more zonally symmetric than the ASH analyses and do not have the same large height gradients from 45° to 65°S. Both the GFDL and ASH analyses compare well against the WMO station reports, with differences typically less than 10 gpm and of the same order as the differences of the station data between the two ten-year periods given in Fig. 3c.

The GFDL and ASH analyses for temperature at 850 mb and the corresponding difference map are shown in Fig. 7. The GFDL analyses are warmer in the regions of high topography in Antarctica and southern Africa due to the different methods of reducing surface observations to pressure levels below the surface. In general, the ASH analyses are much warmer over the oceans (differences up to 7°C), which may be due to a warm bias in the method used to derive the lower-tropospheric guess fields for temperature in the Australian operational analyses (Le Marshall et al., 1985). Both the GFDL and ASH analyses compare reasonably well against the WMO station reports, with differences typically less than 1°C.

The long-term average fields of the GFDL and ASH datasets for summer have been compared in a similar way to those for winter. Since most of the findings for both seasons are qualitatively similar, the presentation of the summer results is confined to showing the difference maps for the zonal and meridional wind at 200 mb, geopotential height at 500 mb and temperature at 850 mb. These maps are shown in Fig. 8.

The largest differences for the zonal wind in summer are due to the weaker high-latitude jet stream in the GFDL analyses, and those for the meridional wind are due to the weaker, more zonally symmetric GFDL analyses. The differences between the geopotential height field at 500 mb in the two analyses are large over the oceans, with weaker gradients from 30° to 60°S in the GFDL analyses. The differences in temperature at 850 mb are due to the high topography over Antarctica and southern Africa and the warmer ASH analyses over the oceans.

b. Latitude-pressure distributions

In this section, the GFDL and ASH analyses for the zonal mean, standing wave variance and covariance statistics for the long-term average fields are presented using latitude–pressure sections. In this study, the long-term average fields for each season were computed first and then the zonal mean, standing wave variance and covariance statistics were calculated. The symbols to be used here have their conventional meaning; $\bar{X}$ time mean, $[X]$ zonal mean and X^* deviation from zonal mean.

In Fig. 9 are shown the zonally averaged distributions for winter of (a) the zonal wind $[\bar{u}]$, (b) meridional wind $[\bar{v}]$, (c) geopotential height $[\bar{z}]$, and (d) temperature $[\bar{T}]$. For each parameter, the fields corresponding to the GFDL analyses, ASH analyses and the difference between the two datasets are displayed in the left, middle and right panels, respectively.

The zonal mean eastward flow in the GFDL analyses is weaker at the mean jet (up to 6 m s^{-1}) and at 55°S (up to 8 m s^{-1}), where a high-latitude jet was found in the ASH analyses. This can be accounted for by the too weak zonal flow in the GFDL analyses over the oceans. The GFDL analyses for meridional wind yield a very strong zonal mean meridional circulation, about three times stronger than in the NH winter (Lau and Oort, 1981), while the ASH analysis is weaker than in the NH winter. It is likely that the sparse conventional observation network and the use of the zonal mean as first guess in the GFDL analyses has led to a marked overestimate of the strength of the zonal mean meridional flow. The ASH analyses for the zonal mean meridional flow have a direct Hadley circulation extending

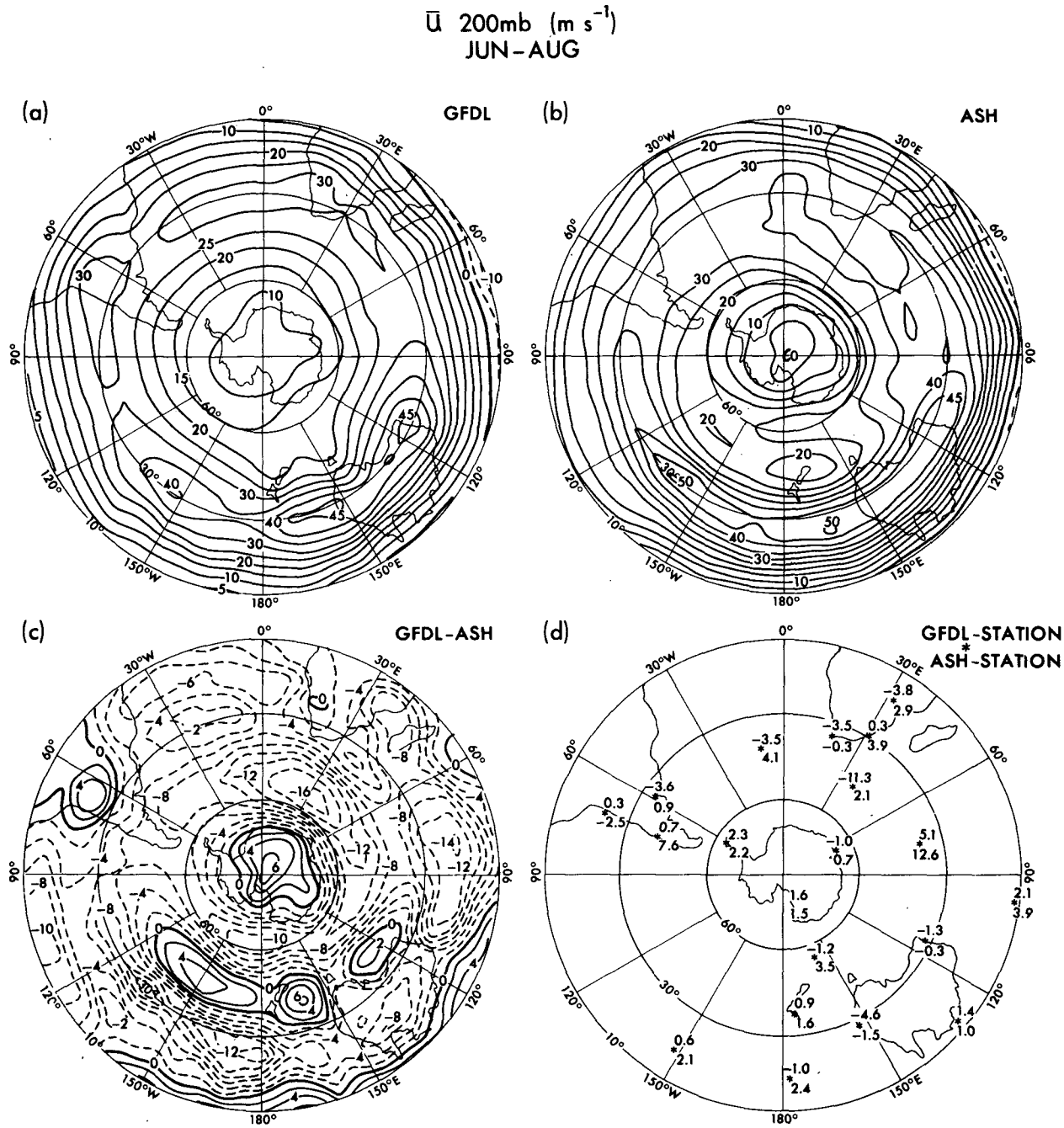

FIG. 4. Distributions of the 10-winter (JJA) average of the zonal wind (m s^{-1}) at 200 mb, based on (a) GFDL and (b) ASH analyses. The difference map in (c) shows the pattern obtained by subtracting the ASH analysis from the GFDL analysis. The values computed by subtracting the long-term mean WMO station data from the GFDL (ASH) analyses are displayed above (below) the location of the individual stations in (d).

to about 20°S, an indirect Ferrel cell in middle latitudes and a direct polar cell. This zonal-mean meridional flow is similar in SH middle latitudes to that from the FGGE analyses (Lau, 1984) but it is much weaker in low latitudes than from FGGE. The meridional flow at low latitudes in the ASH analyses is limited by the operational constraint to the climatological wind field of Taljaard et al. (1969). The zonal-mean geopotential height has a stronger gradient in the ASH analyses from 30° to 60°S, but a weaker gradient from 60°S to the pole. The differences of zonal-mean zonal wind in Fig. 9a are not in geostrophic balance with the meridional

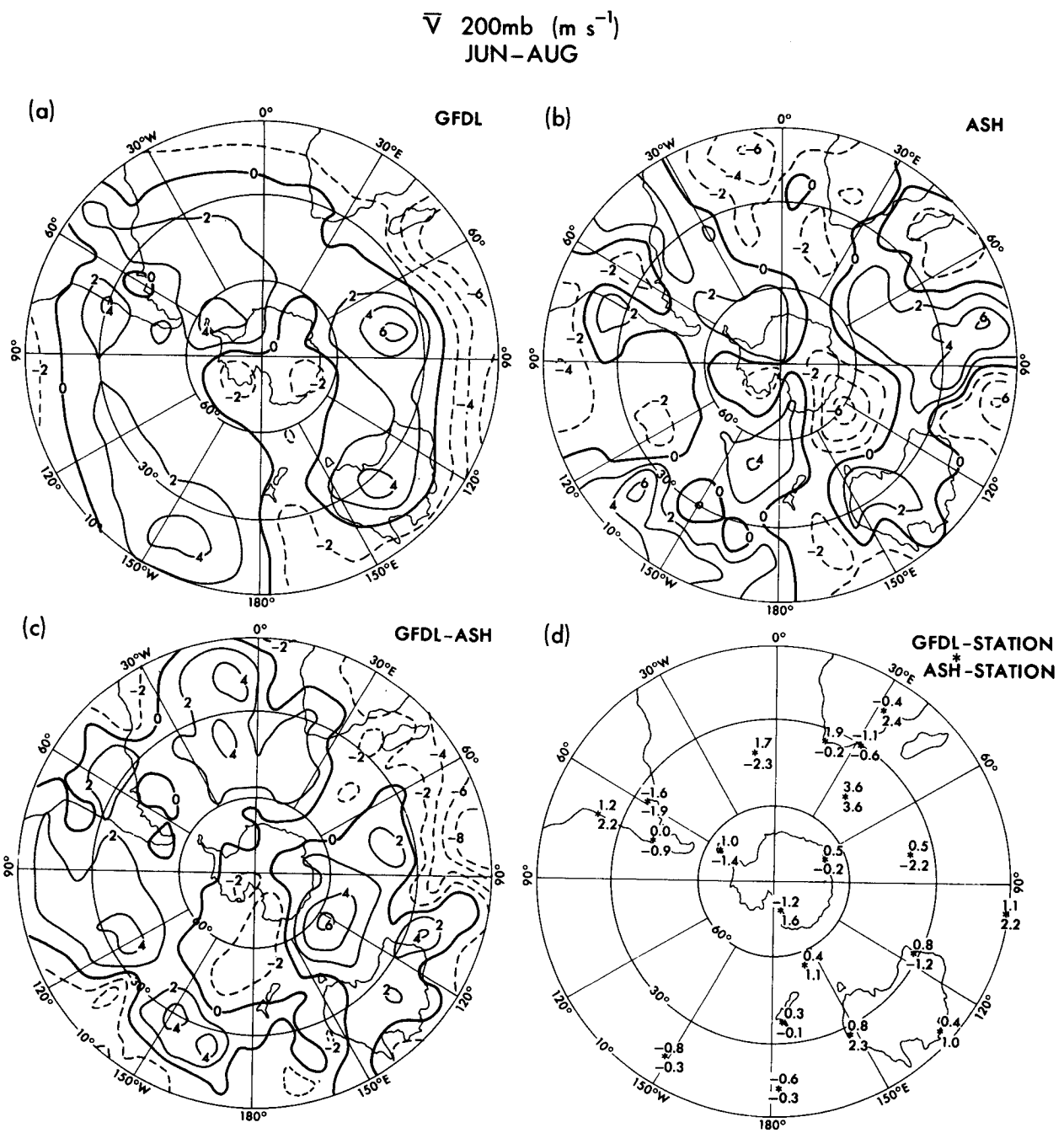

FIG. 5. As in Fig. 4 except for meridional wind speed (m s^{-1}) at 200 mb.

gradient of the differences of zonal-mean height in Fig. 9c. This is due to the absence of any dynamical constraints between the wind and height fields in the GFDL analyses which exist to some extent in the ASH analyses. The higher heights in the ASH analyses at high latitudes may be due in part to trends in the heights between the two time periods (Mo and van Loon, 1984, Swanson and Trenberth, 1981a). The zonal-mean temperatures in the ASH analyses are warmer below 700 mb but the differences are small in the middle troposphere. At high latitudes, the ASH analyses are colder, possibly due in part to a real trend between the two time periods mentioned previously. These differences between the two periods can also be seen in the high-latitude station data in Fig. 3d.

The winter distributions of the root-mean-square standing wave zonal variations of (a) zonal wind, $[\bar{u}^{*2}]^{1/2}$, (b) meridional wind, $[\bar{v}^{*2}]^{1/2}$, (c) geopotential height,

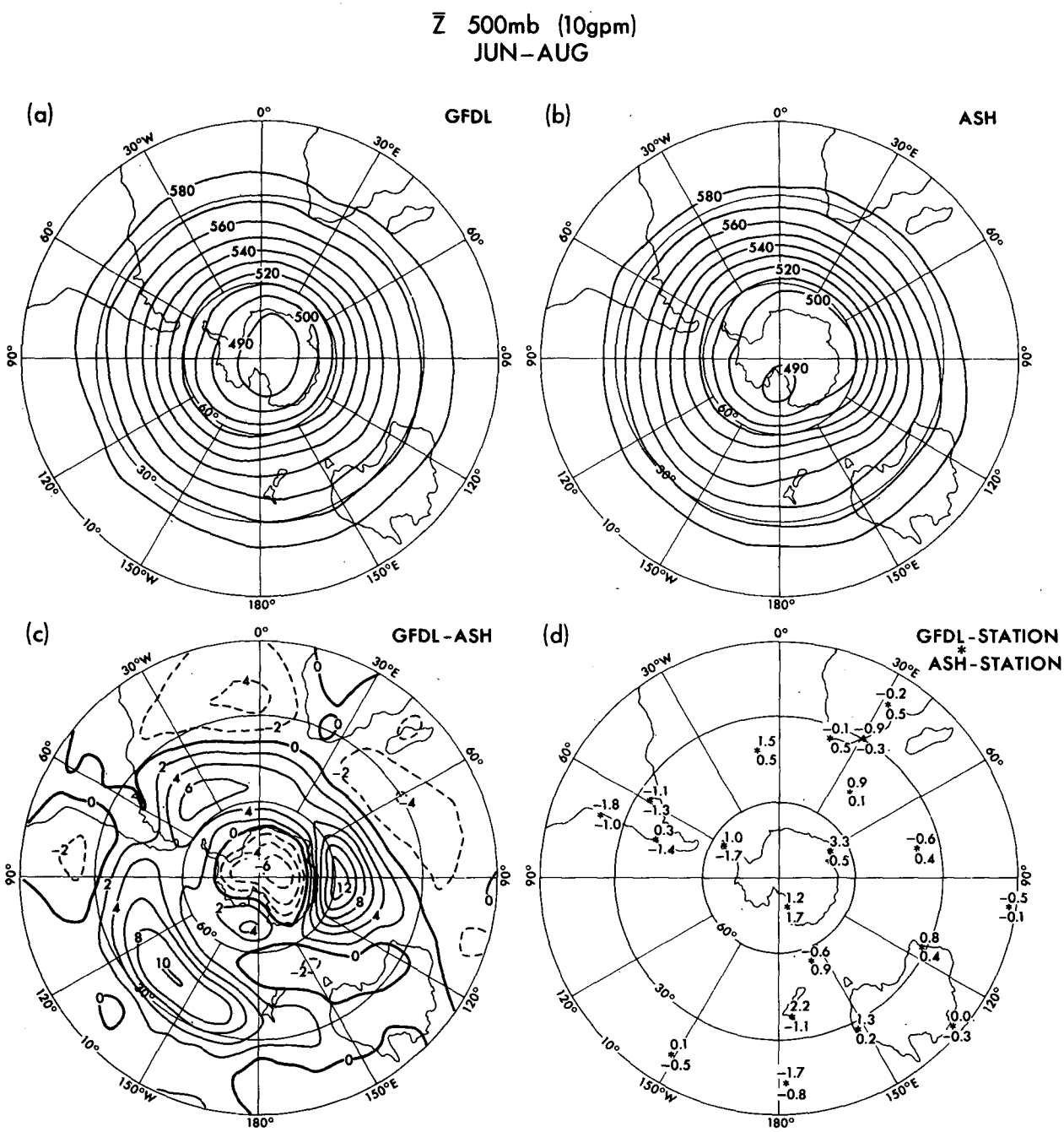

FIG. 6. As in Fig. 4 except for geopotential height (dam, 1 dam = 10 gpm) at 500 mb.

$[\bar{z}^{*2}]^{1/2}$ and (d) temperature, $[\bar{T}^{*2}]^{1/2}$, for the GFDL analyses (left panel), ASH analyses (middle panel) and the corresponding difference (right panel) are shown in Fig. 10. For all these parameters, differences between the two datasets are small from 10° to 30°S. At middle and high latitudes, the standing wave amplitudes are much larger in the ASH analyses. The GFDL analyses have very small zonal variations from 40° to 60°S where there are very few rawinsonde stations. The rms zonal variations from the ASH analyses are similar in distribution but smaller in amplitude in high latitudes than those for the FGGE winter (Lau, 1984).

The standing wave covariance statistics for winter which give the meridional transports of (a) zonal momentum $[\bar{v}^*\bar{u}^*]$ and (b) heat $[\bar{v}^*\bar{T}^*]$ by the standing waves are compared in Fig. 11. The standing wave transports in the SH are much smaller than in the NH (Obasi, 1963, Trenberth, 1981, Karoly, 1985). There

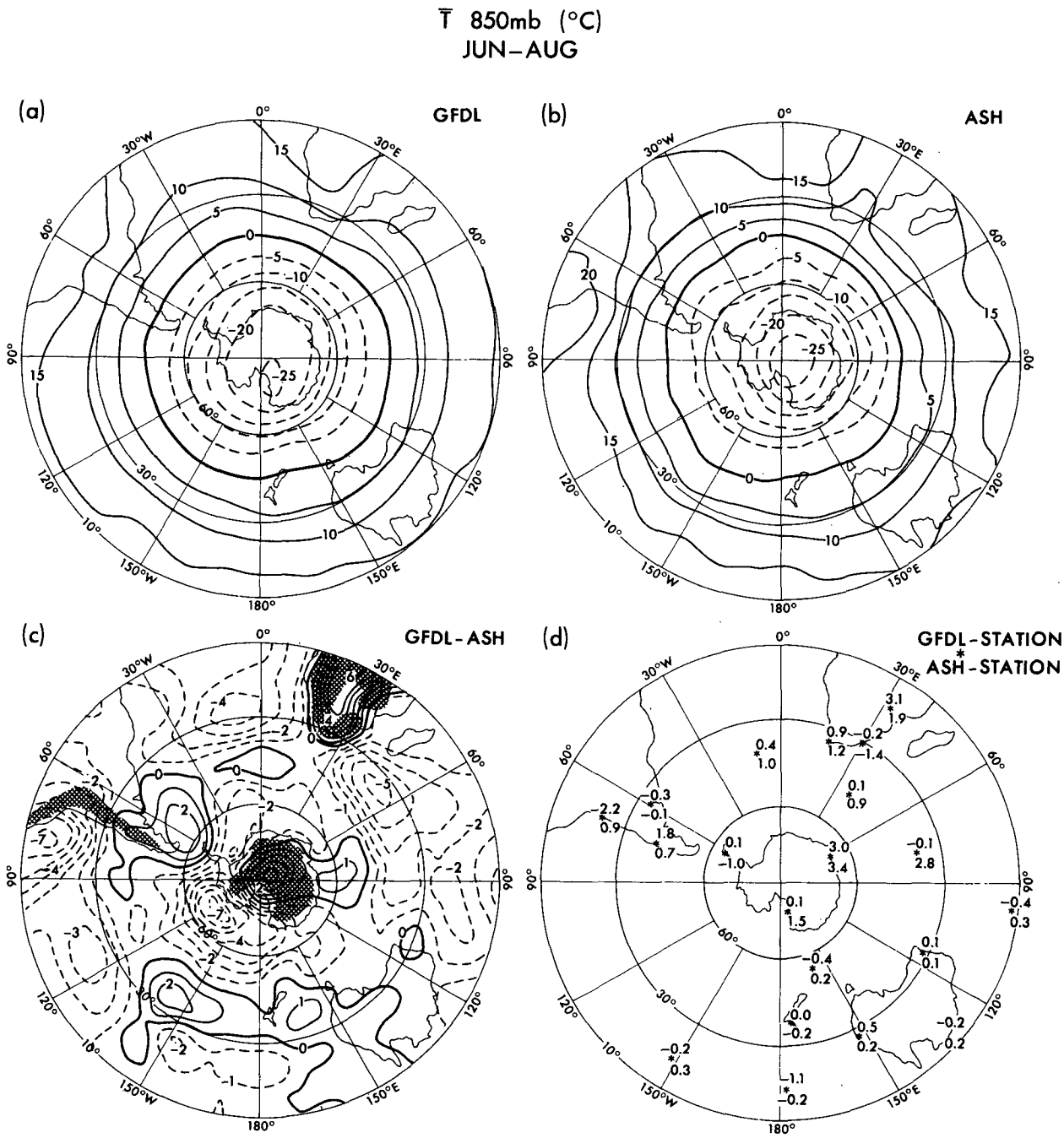

FIG. 7. As in Fig. 4 except for temperature (°C) at 850 mb. Cross-hatching indicates regions where the 850-mb level is below the surface.

are broad similarities between the standing wave transports in the two datasets but the values tend to be small so that the differences between the two datasets (not shown) are comparable to the analysed transports. The possible errors in the long-term average fields in the two datasets are large enough to have made significant erroneous contributions to these transports. These standing wave transports therefore are unreliable. The amplitudes of the SH standing wave transports during the FGGE winter (Lau, 1984) are also small.

4. Daily transient eddy statistics

In this section, the GFDL and ASH analyses for the long-term average standard deviation and covariance of daily fluctuations are compared. As described in

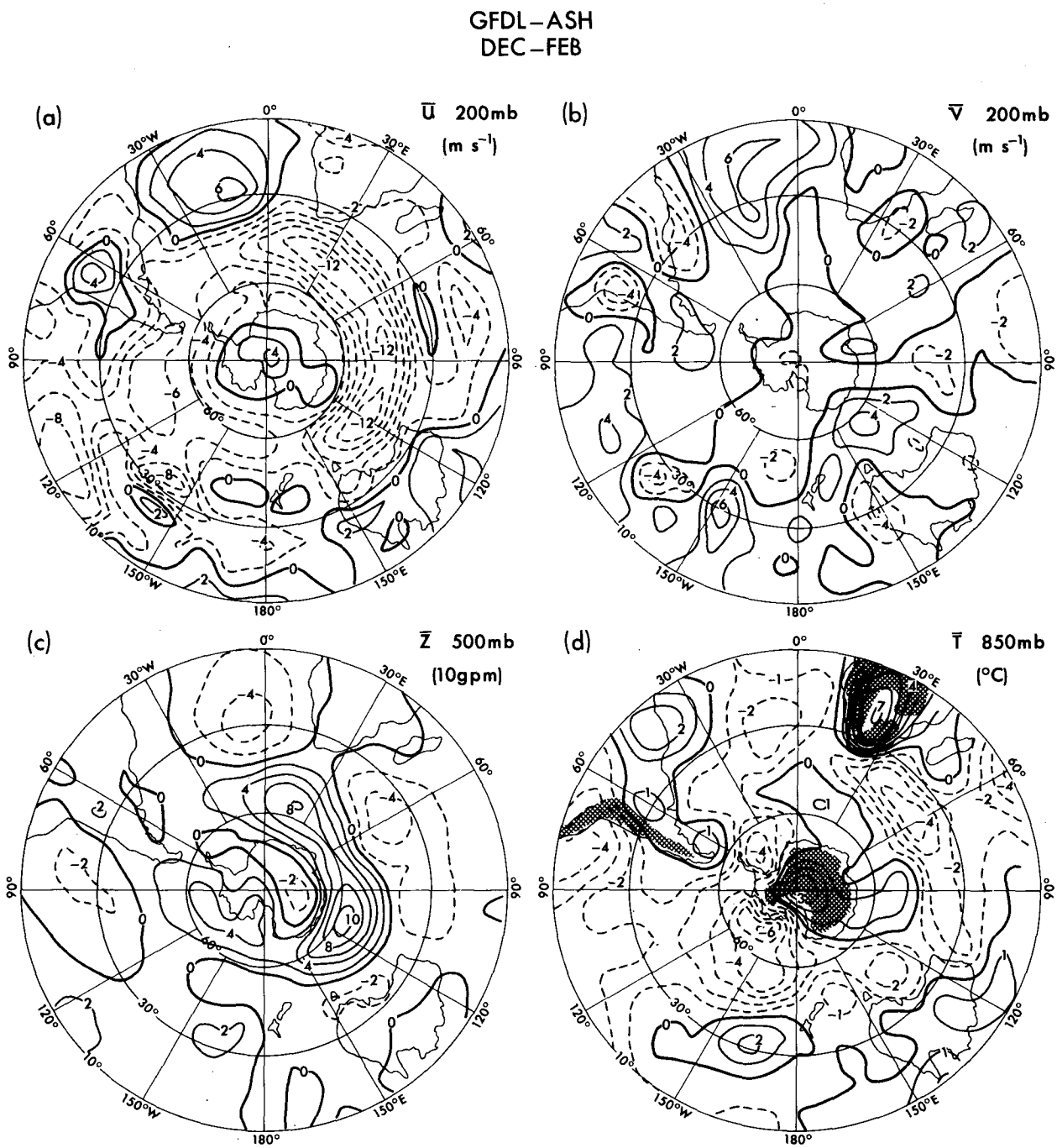

FIG. 8. Difference maps obtained by subtracting the ASH analysis from the corresponding GFDL analysis, based on the 10-summer (DJF) averages of (a) zonal wind (m s^{-1}) at 200 mb, (b) meridional wind (m s^{-1}) at 200 mb, (c) geopotential height (dam) at 500 mb and (d) temperature (°C) at 850 mb.

section 2, a different method was used in each dataset for the calculation of the long-term average standard deviations which should lead to a small, systematic increase in the GFDL values over the ASH values. This difference is likely to be smaller than those due to other causes and will be ignored in the following comparisons.

a. Hemispheric distributions

The distributions of winter daily transient-eddy kinetic energy $(\overline{u'^2} + \overline{v'^2})/2$, at 200 mb based on GFDL and ASH analyses and the corresponding difference are shown in Fig. 12. There is good agreement between the spatial patterns in the GFDL and ASH analyses

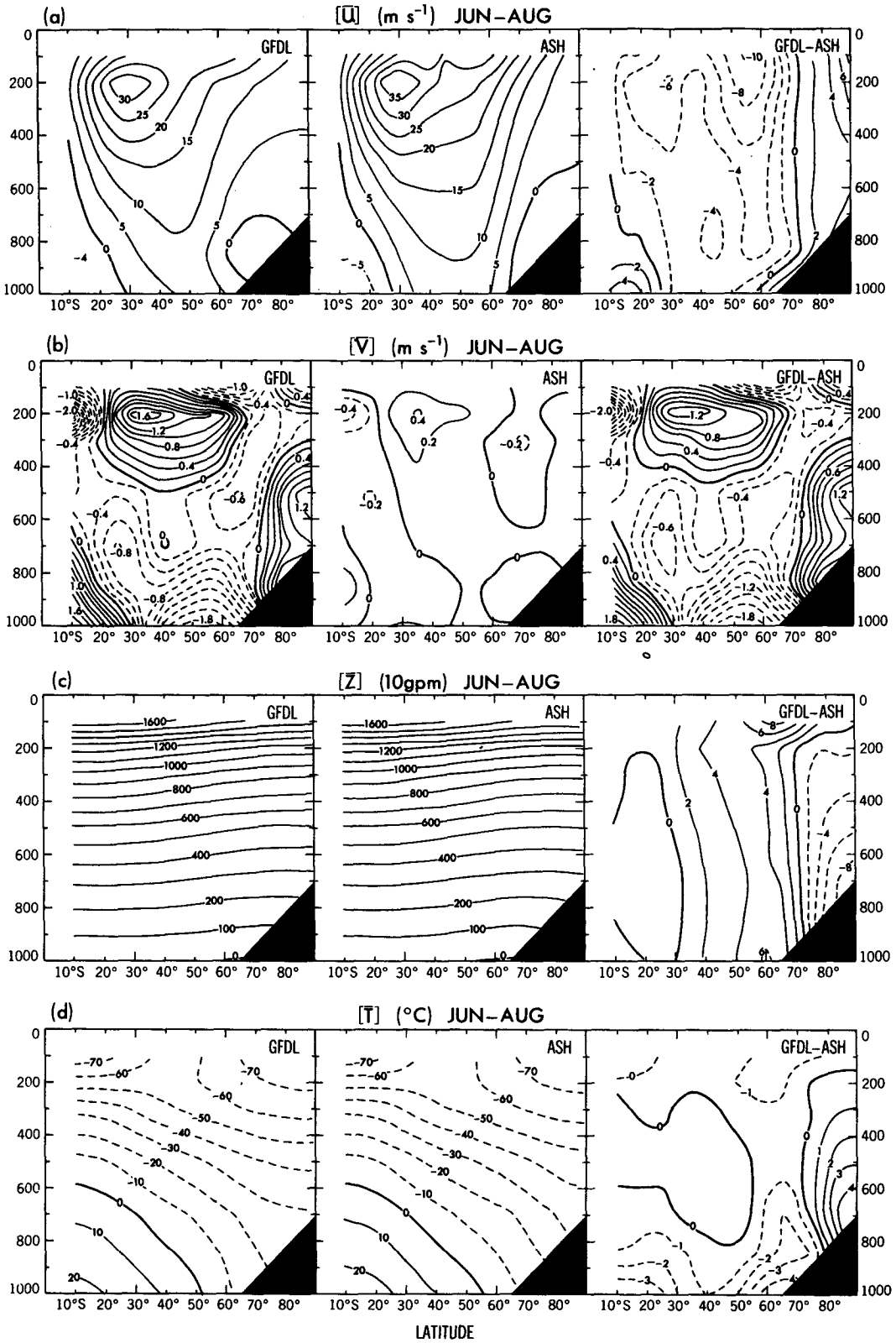

FIG. 9. Meridional cross sections of the zonal mean of (a) the zonal wind (m s^{-1}), (b) meridional wind (m s^{-1}), (c) geopotential height (dam) and (d) temperature (°C), based on the 10-winter averages of the GFDL analyses (left panel) and ASH analyses (middle panel). The differences between the two sets (GFDL-ASH) are shown in the right panel. The dark region in the lower right-hand corner of the section indicates the region below the surface of Antarctica.

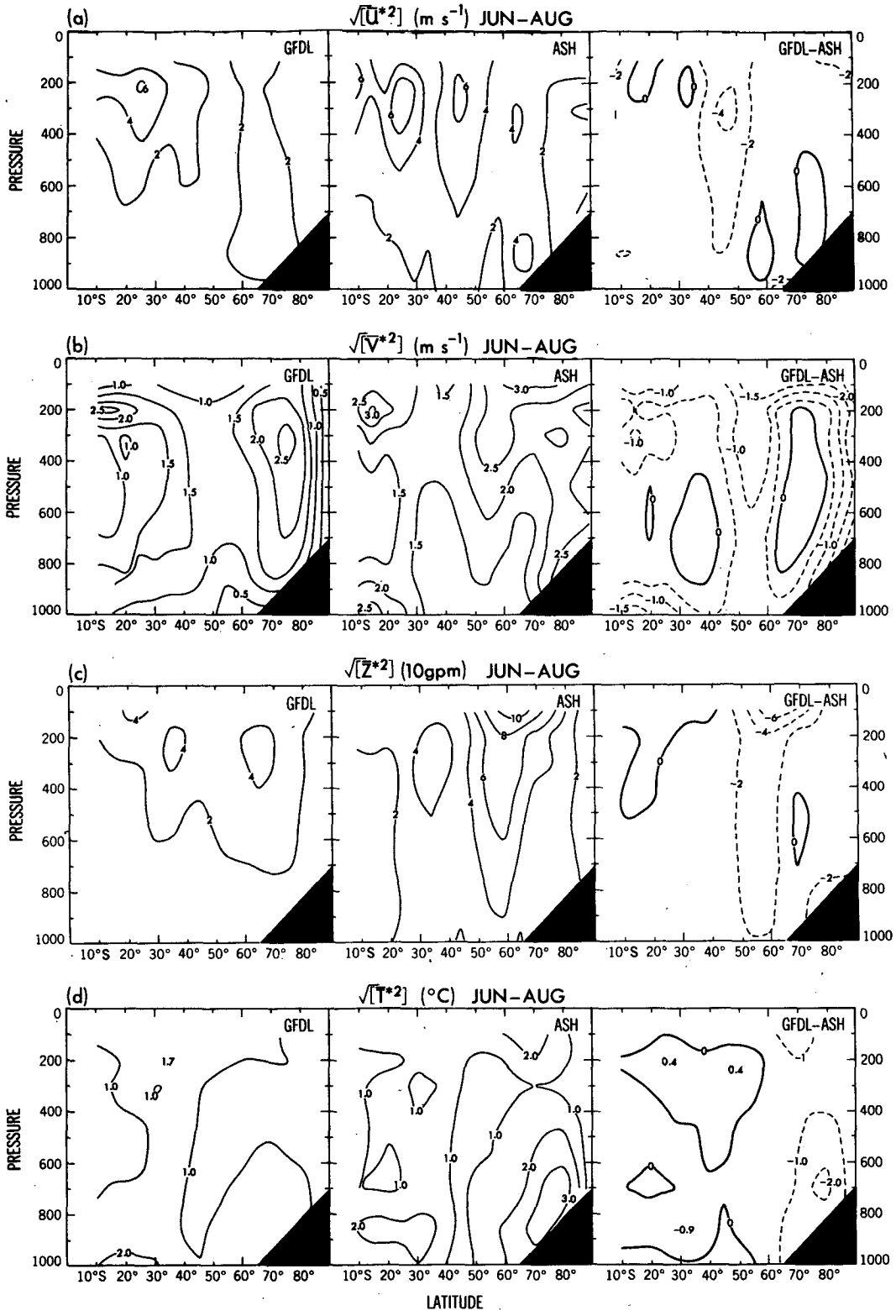

FIG. 10. As in Fig. 9 except for winter root-mean-square zonal variations of (a) zonal wind (m s^{-1}), (b) meridional wind (m s^{-1}), (c) geopotential height (dam) and (d) temperature (°C).

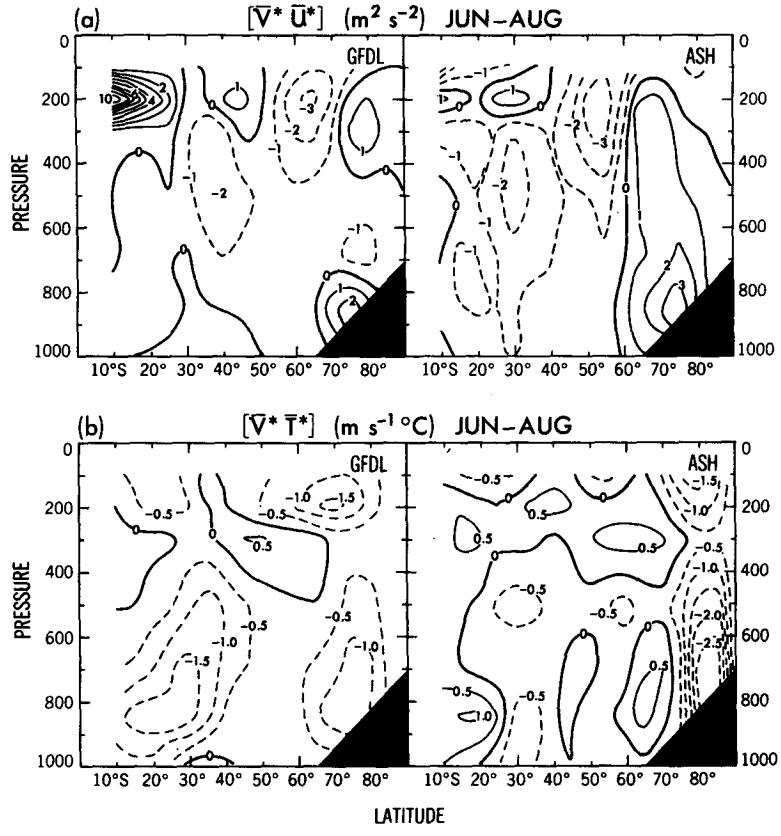

FIG. 11. As in Fig. 9 except for the winter standing-wave meridional transports of (a) westerly momentum ($m^2 s^{-2}$) and (b) heat (°C m s^{-1}). The differences between the two datasets are not shown.

over much of the SH, better than for the mean fields. However, the amplitude of the transient kinetic energy is larger by about 20% in the GFDL analyses. The GFDL analyses also have a smoother spatial structure. The largest differences occur at low latitudes, where the variability of the wind field in the ASH analyses is reduced by the climatological constraint in the operational analysis procedure.

The distributions of the daily standard deviation of geopotential height, $(\overline{z'^2})^{1/2}$, at 500 mb are compared in Fig. 13. The two sets are in good agreement from 10° to 30°S, with the GFDL analyses having slightly larger values (differences < 10 gpm). At higher latitudes, where both analyses have their maxima and where there are very few rawinsonde stations, the amplitude of the height fluctuations in the ASH analyses is larger by up to 20 gpm and the GFDL analyses are smoother.

The GFDL and ASH analyses of the daily standard deviation of temperature, $(\overline{T'^2})^{1/2}$, at 850 mb are shown in Fig. 14. The fields are broadly similar, with a smoother pattern and larger values in the GFDL analysis (up to 1.5°C). The largest differences occur over the Atlantic and Indian Oceans and below the surface of Antarctica.

In general, the features noted above for winter are also found in summer and the difference maps for summer are not shown here. The transient eddy kinetic energy in summer at 200 mb is slightly larger in the GFDL analyses, the transient height fluctuations at 500 mb are larger in the ASH analyses at high latitudes and the transient temperature fluctuations at 850 mb are larger in the GFDL analyses.

The distribution of the winter meridional transport of momentum by the transient eddies, $\overline{v'u'}$, at 200 mb based on the GFDL and ASH analyses and the corresponding difference is shown in Fig. 15. The general spatial pattern for the momentum flux is similar for the two sets of analyses, with the ASH analyses having stronger poleward fluxes in middle latitudes and more small-scale variations.

The distributions of the winter transport of heat by the transient eddies, $\overline{v'T'}$, at 850 mb are compared in Fig. 16. Again the fields are similar in terms of the broad patterns, but here the GFDL analyses have larger values and a smoother pattern than the ASH analyses.

b. Latitude–pressure distributions

Figure 17 shows the meridional distributions of the winter zonal means of (a) transient kinetic energy

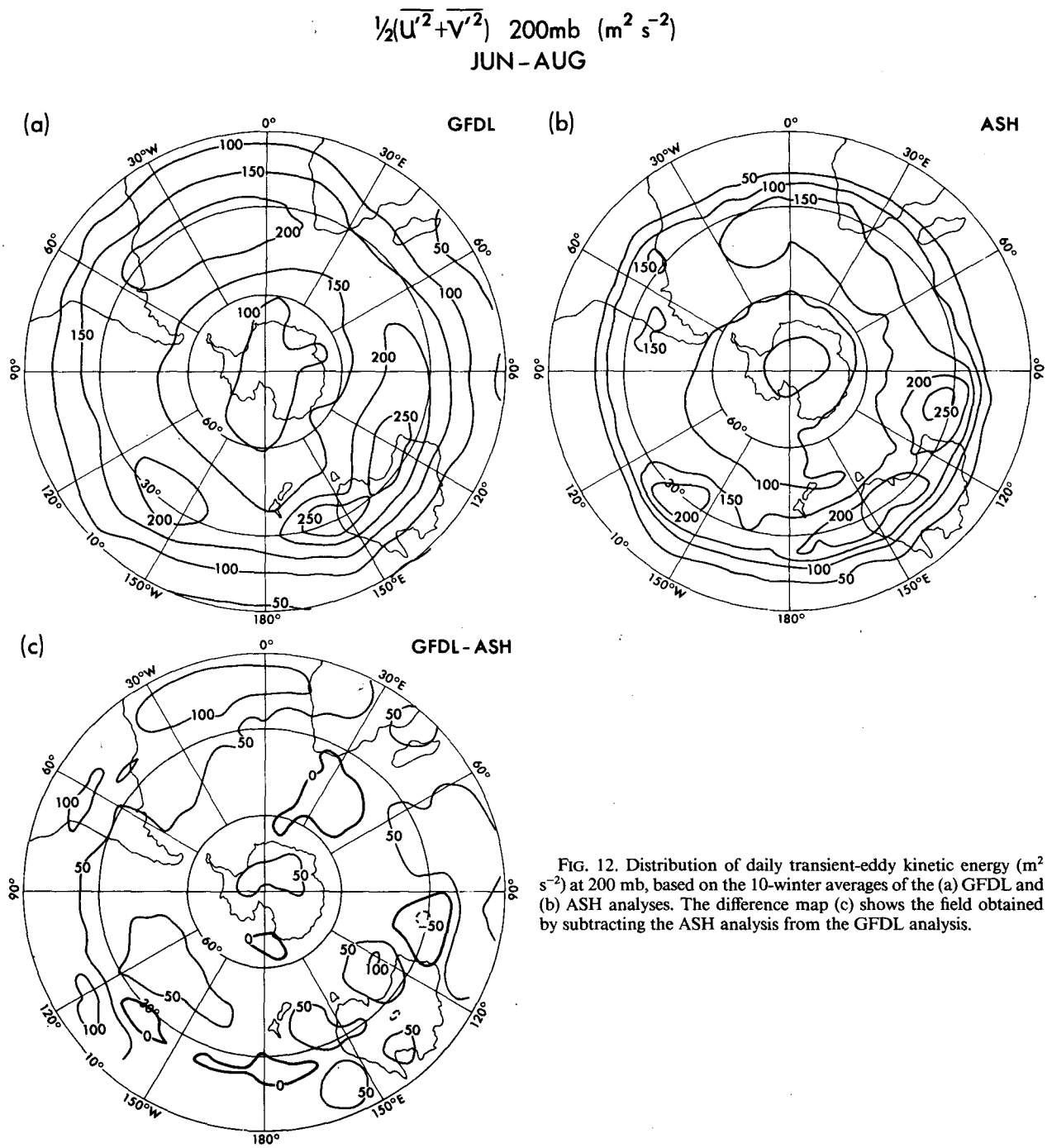

FIG. 12. Distribution of daily transient-eddy kinetic energy (m^2 s^{-2}) at 200 mb, based on the 10-winter averages of the (a) GFDL and (b) ASH analyses. The difference map (c) shows the field obtained by subtracting the ASH analysis from the GFDL analysis.

$[(\overline{u'^2} + \overline{v'^2})/2]$, (b) daily standard deviation of geopotential height $[(z'^2)^{1/2}]$, and (c) daily standard deviation of temperature $[(\overline{T'^2})^{1/2}]$ for the GFDL analyses (left panel), ASH analyses (middle panel) and the corresponding differences (right panel). There is reasonably good agreement between the two datasets for the vertical structure of the zonal mean of the transient variations. The amplitudes of the transient kinetic energy and temperature fluctuations in the upper troposphere are much larger in the GFDL analyses, while in the middle and lower tropospheres, the amplitudes are similar. The values from the FGGE analyses (Lau, 1984) are closer to those from the GFDL analyses although the GFDL values are larger at the tropopause level.

The winter zonal mean distributions of the meridional transport by the transient eddies are compared in Fig. 18 for (a) zonal momentum, $[\overline{v'u'}]$, and (b) heat,

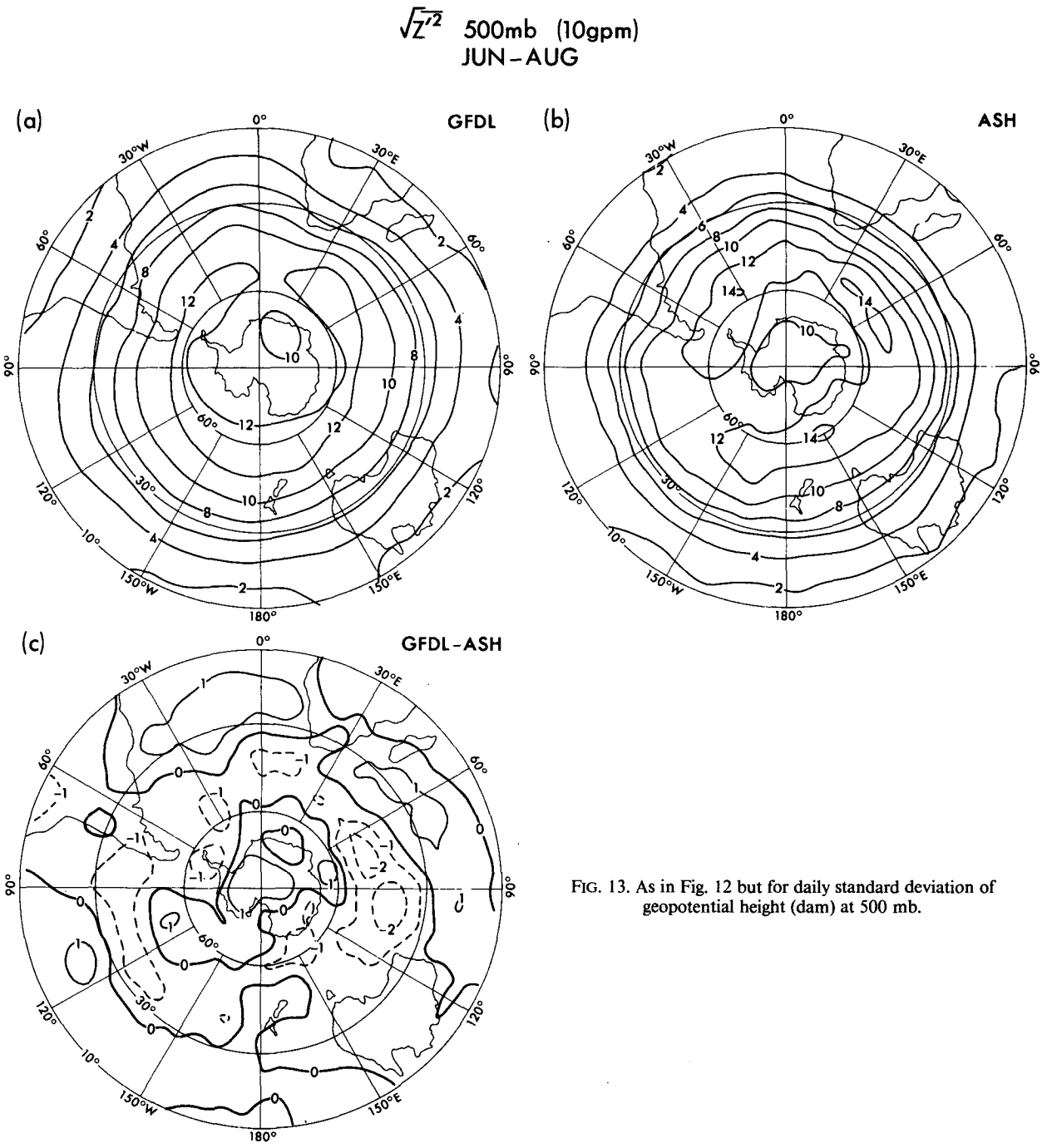

FIG. 13. As in Fig. 12 but for daily standard deviation of geopotential height (dam) at 500 mb.

$[\overline{v'T'}]$, from the GFDL analyses (left panel), ASH analyses (center panel) and the corresponding differences (right panel). There is reasonable agreement between the two datasets for the momentum transport, with larger equatorward flux at high latitudes in the GFDL analyses. In the upper troposphere at middle latitudes, the poleward momentum flux is similar in magnitude even though the transient kinetic energy from the ASH analyses was much smaller than from the GFDL analyses. The vertical structure of the heat transport from the ASH analyses has some unusual features with almost no vertical variation between 850 and 500 mb, too small transport at low levels and weak equatorward rather than poleward transport at the tropopause level at middle and high latitudes. This reversed heat transport in the ASH analyses in the upper troposphere has been noted by van Loon (1980) for the ASH analyses prior to 1979, the year of the Global Weather Exper-

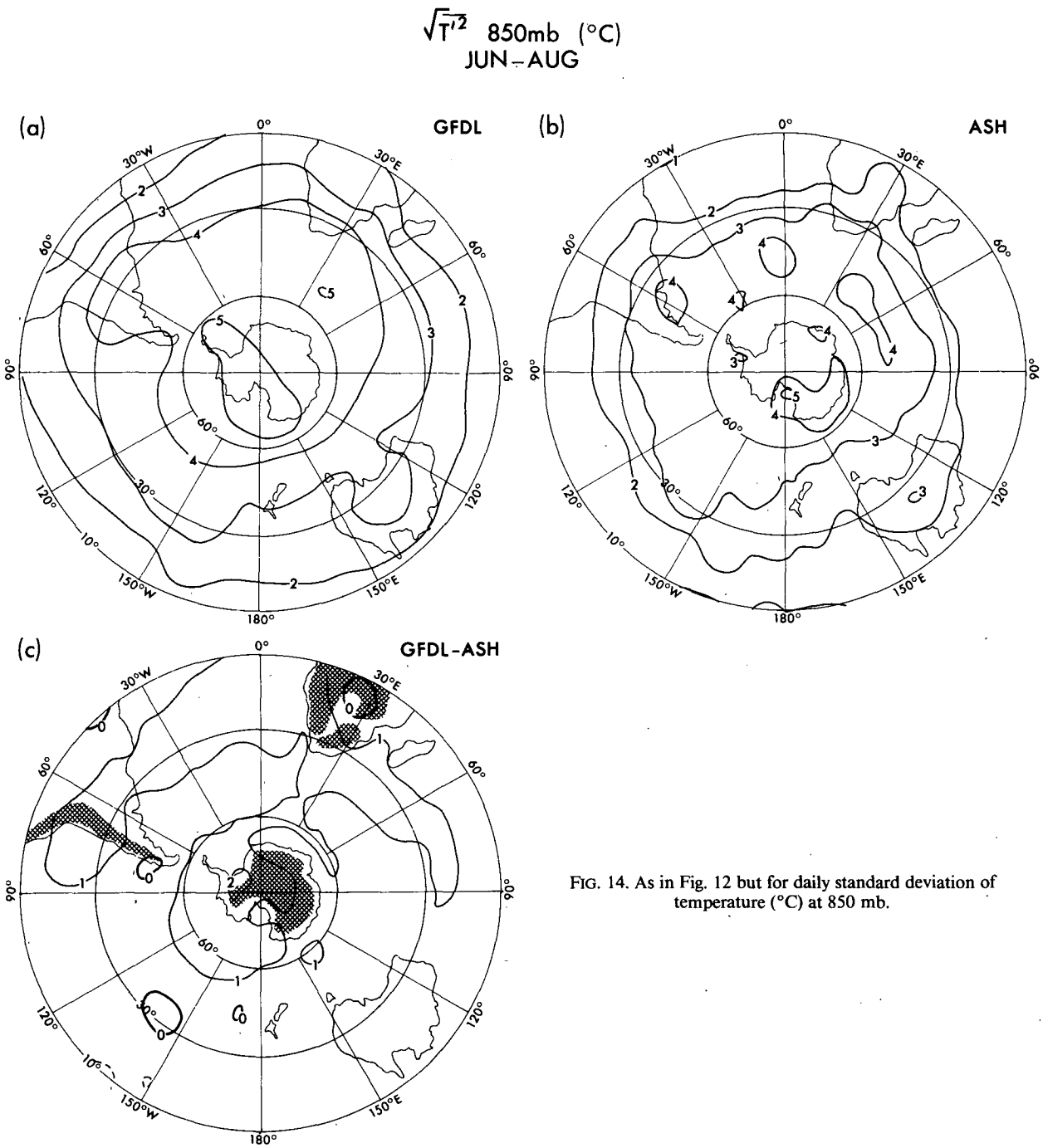

FIG. 14. As in Fig. 12 but for daily standard deviation of temperature (°C) at 850 mb.

iment, but it is also apparent for the period after 1979. This seems to be an artifact of the ASH analysis system which affects the phase of the transient fluctuations of wind and temperature in the upper troposphere. Again, the values from the FGGE analyses are closer to those from the GFDL analyses for both the momentum and heat transport, indicating that the heat transport in the upper troposphere of the ASH analyses is incorrect.

5. Interannual variability of the monthly mean fields

In this section, the GFDL and ASH analyses for the standard deviation of the monthly mean fields are presented. The seasonal cycle was removed by subtracting the ten-year average for each calendar month from the individual monthly means to give monthly departures. The standard deviation of the monthly departures, $\sigma(X)$, was then calculated.

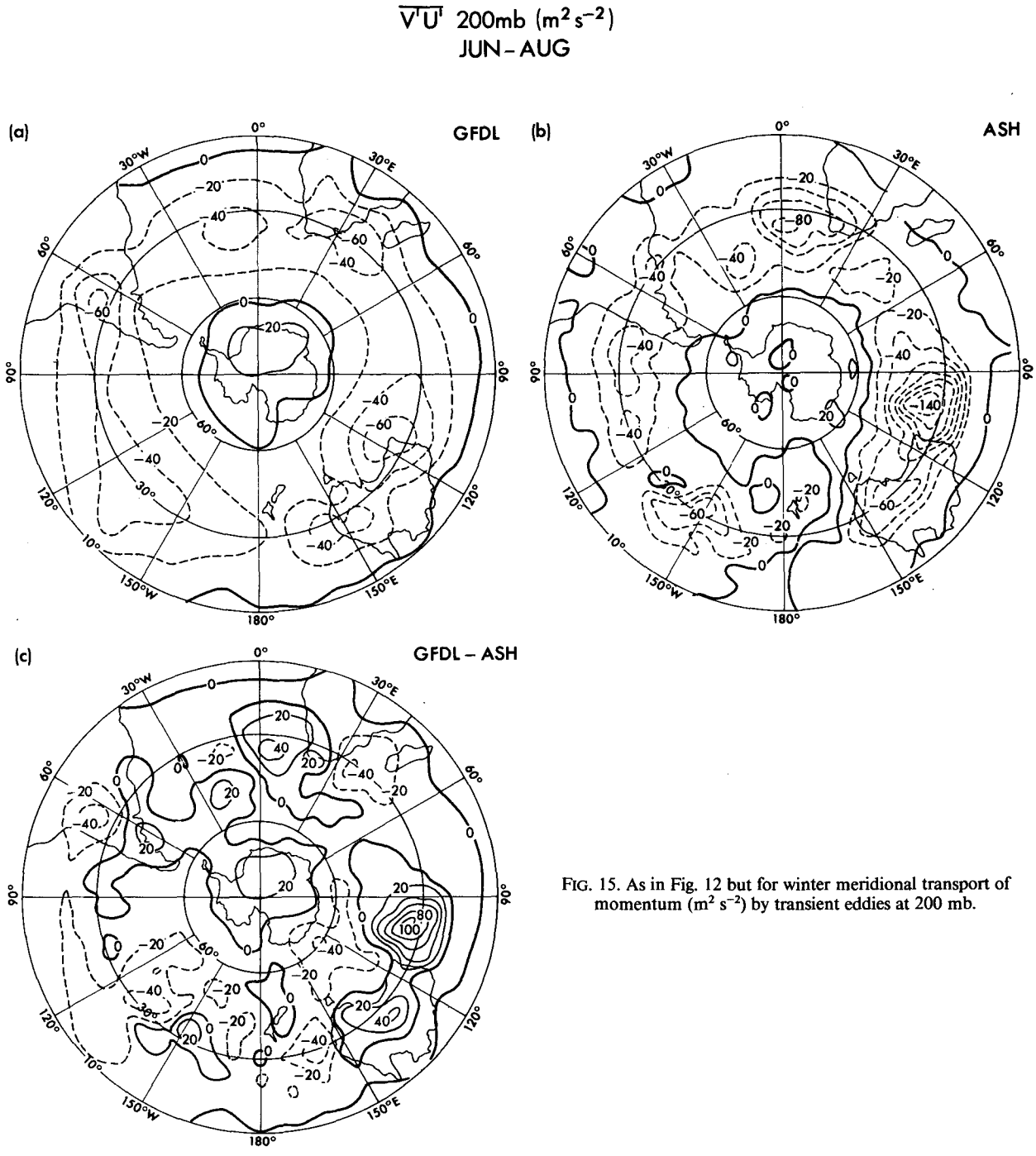

FIG. 15. As in Fig. 12 but for winter meridional transport of momentum ($m^2 s^{-2}$) by transient eddies at 200 mb.

a. Hemispheric distributions

The distribution of the standard deviation of the winter monthly mean zonal wind, $\sigma(u)$, at 200 mb from the GFDL and ASH analyses and the corresponding difference map are shown in Fig. 19. There is some agreement between the two datasets for the overall pattern, but the features in the ASH analyses are more clearly defined, particularly the maxima in the jet-exit region over the Pacific Ocean and the high-latitude jet over the Southern Ocean. The largest differences (up to 4 m s^{-1}) occur at low latitudes where the variability of the monthly mean winds in the ASH analyses is reduced by the climatological constraint in the operational analysis procedure.

The standard deviations of the monthly mean ra-

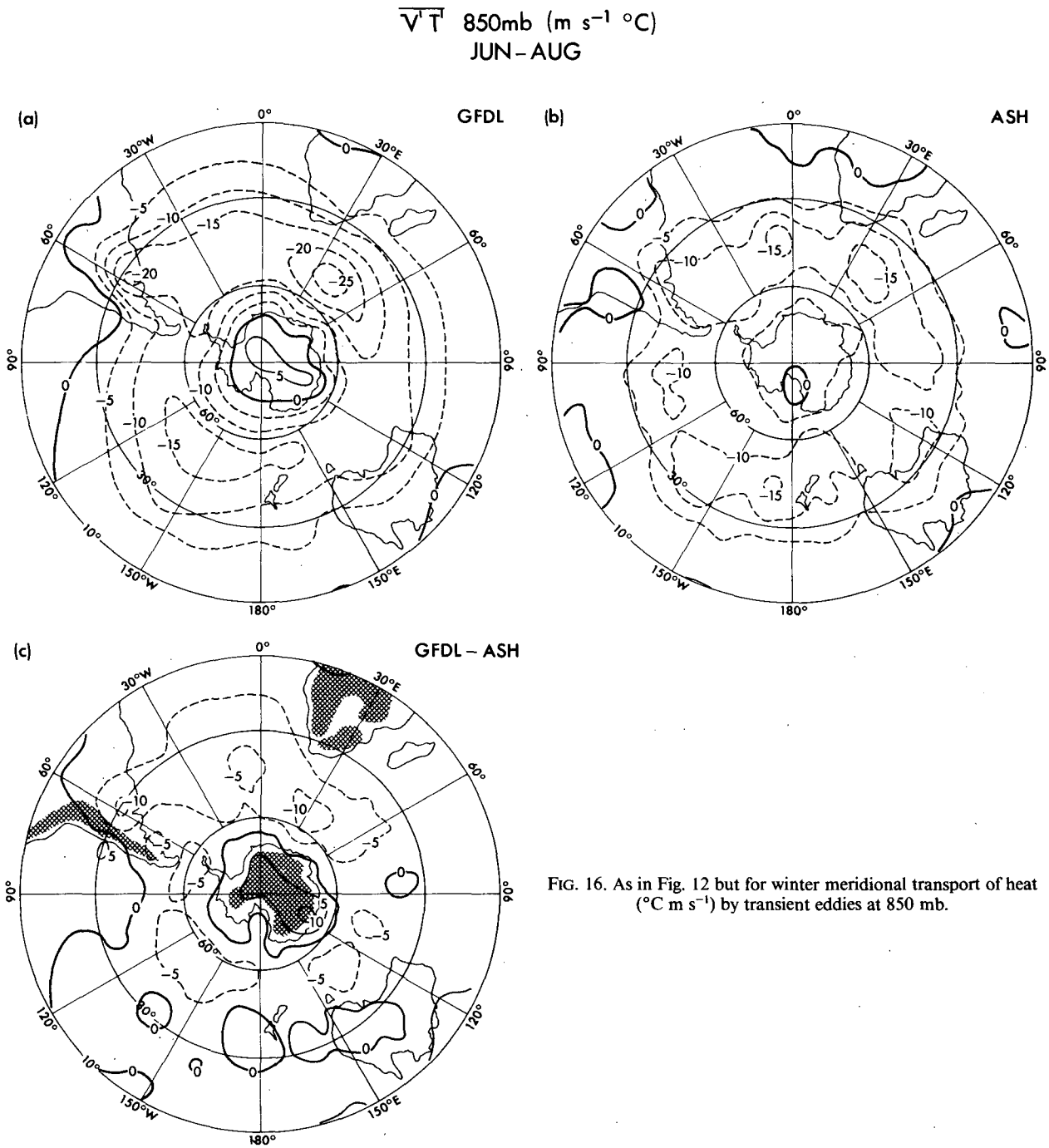

FIG. 16. As in Fig. 12 but for winter meridional transport of heat (°C m s^{-1}) by transient eddies at 850 mb.

winsonde station observations have been computed using the available data for the 20 WMO stations in Table 1 over the full 20-year period 1960–79. The differences of the GFDL (ASH) analyses minus the WMO station value for the monthly standard deviation have been plotted above (below) the station location in Fig. 19d and can be used as a check on the analyses. In general, the three datasets agree well at the station locations, except over southern Africa and the nearby island stations where the analyses have smaller variability. In general, the ASH analyses have smaller values than the GFDL analyses even at the station locations.

The standard deviation of the monthly mean meridional wind, $\sigma(v)$, at 200 mb shows many similar features to those for the zonal wind, with smoother

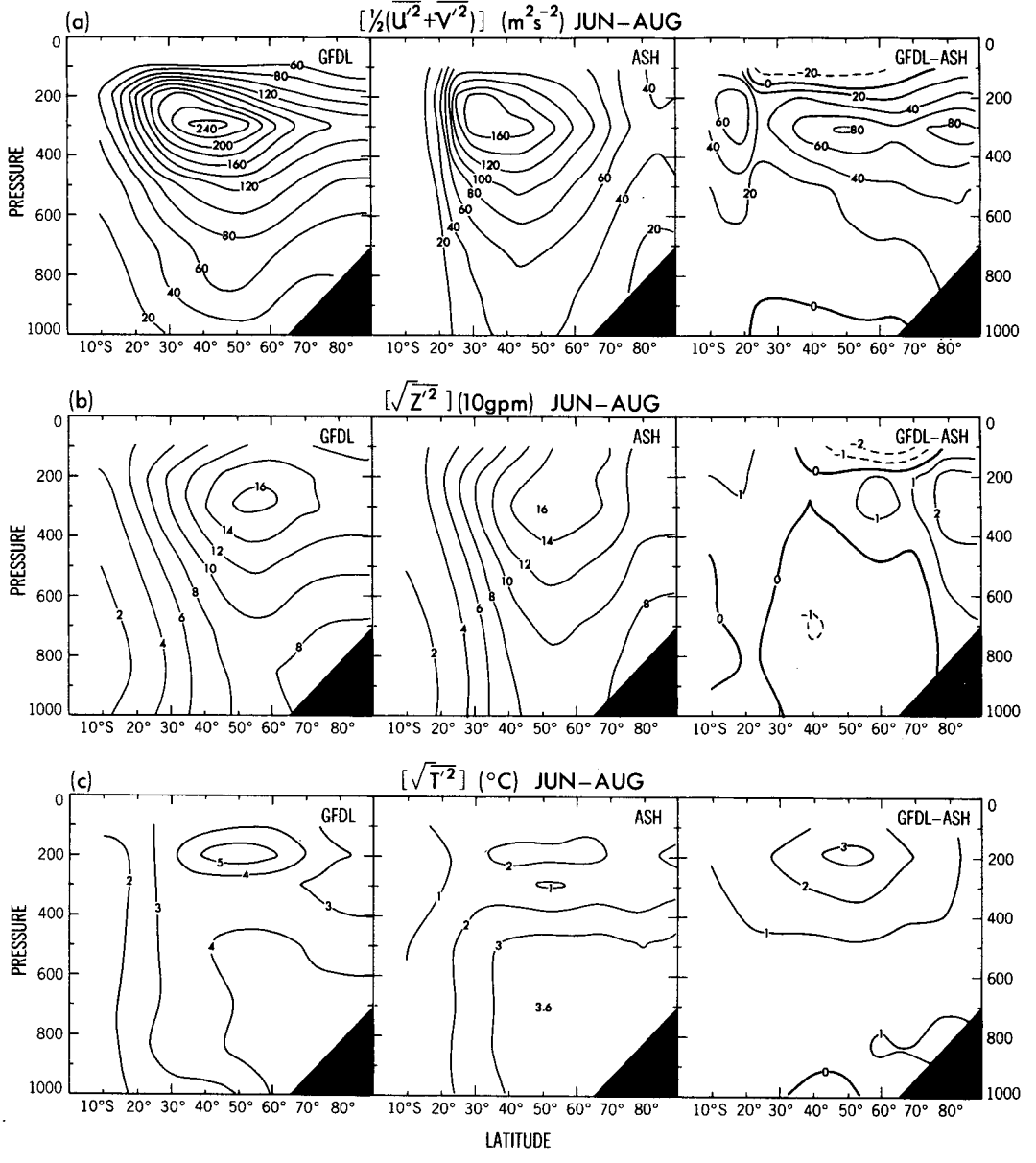

FIG. 17. Meridional cross sections of the winter zonal mean of (a) daily transient kinetic energy ($m^2 s^{-2}$), (b) daily standard deviation of geopotential height (dam) and (c) daily standard deviation of temperature (°C), based on the 10-winter averages of the GFDL analyses (left panel) and ASH analyses (middle panel). The differences between the corresponding fields from the two sets are shown in the right panel.

fields and generally larger values in the GFDL analyses, but the corresponding maps are not shown here.

The GFDL and ASH analyses for the standard deviation of the monthly mean geopotential height, $\sigma(z)$, at 500 mb in Fig. 20 are broadly similar, with a smoother field in the GFDL analyses but with differences less than about 10 gpm over most of the SH. At the station locations, the two datasets agree well with the WMO station data.

The patterns for the variability of the monthly mean temperature at 850 mb are not shown but they are similar for the two datasets except over Antarctica, where the 850 mb level is below the surface and where there are marked trends in temperature in the ASH analyses, and over the eastern equatorial Pacific Ocean, a region with no radiosonde stations. The larger variability in the ASH analyses in this region may be due to the impact on the analyses of satellite-derived temperature retrievals. The two datasets agree well with the WMO station data.

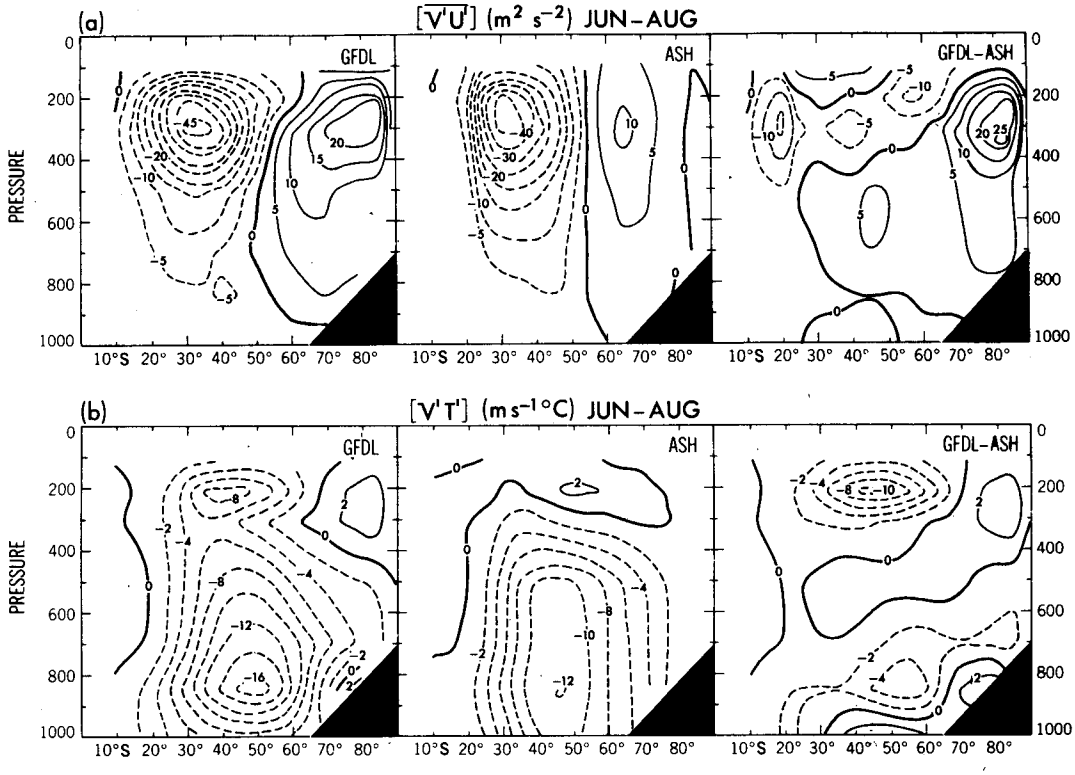

FIG. 18. As in Fig. 17 except for winter zonal mean meridional transport of (a) momentum ($m^2 s^{-2}$) and (b) heat (°C m s^{-1}) by transient eddies.

b. Latitude–pressure distributions

The meridional distributions of the zonal-mean winter standard deviations of monthly mean (a) zonal wind [$\sigma(u)$], (b) meridional wind [$\sigma(v)$], (c) geopotential height [$\sigma(z)$], and (d) temperature [$\sigma(T)$] based on the GFDL analyses (left panel), ASH analyses (middle panel) and the corresponding difference (right panel) are presented in Fig. 21. The distributions from the two datasets agree well, with larger amplitude variability in the GFDL dataset at the tropopause level, especially for meridional wind and temperature, and at low latitudes for both zonal and meridional wind.

6. Conclusions

It should be emphasized that, on the basis of the present comparison, each of the datasets has its advantages and disadvantages and it is not possible to decide which set of analyses is better than the other, in an overall sense. It is possible, however, to point out some of the obvious deficiencies and to suggest a better composite set of circulation statistics for the SH. Judging from the results presented so far, it is felt that the following assessment of the relative merits of the GFDL and ASH datasets may be made:

a. The time-mean fields

The differences of the mean fields between the two datasets are large away from radiosonde station locations. Some indication of whether these differences may be due to the different time periods used for the averages can be obtained by estimating the standard deviation of ten-year means from the interannual variability of the monthly mean fields presented in section 5. Dividing the standard deviation of the monthly means by the square root of ten, the number of years in the average, gives a rough estimate of the standard deviation of the ten-year means. Since the largest differences of the mean fields between the two datasets are much larger than three times the estimated standard deviation of the ten-year means for all the fields, it is very unlikely that the differences of the mean fields are due to the different time periods used.

The differences between the station means for two ten-year periods shown in Fig. 3 provide a better estimate of the real differences between the two time periods. In data-sparse regions, the differences of the mean fields between the two datasets are much larger than those between the two periods at the stations.

These results show that the differences between the two datasets are not due primarily to the different time periods used for each dataset, but are due to the different analysis methods and the different data sources.

For the time-mean fields, the ASH analyses compare better with the earlier SH climatology of Taljaard et

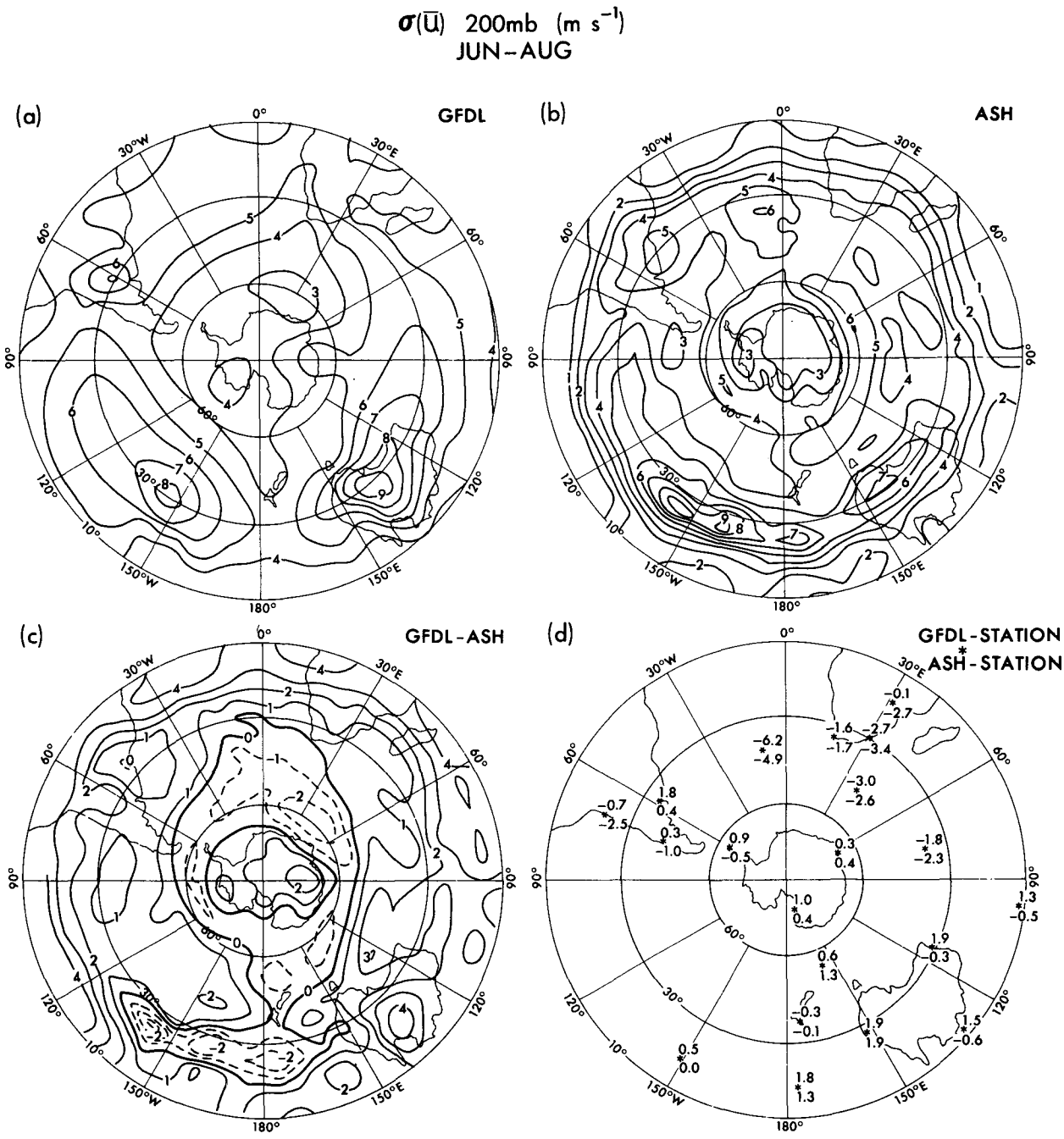

FIG. 19. Winter distribution of the standard deviation of monthly mean zonal wind (m s^{-1}) at 200 mb, based on (a) GFDL analyses and (b) ASH analyses, with the corresponding difference map (GFDL-ASH) shown in (c). The values obtained by subtracting the WMO station data values from the GFDL (ASH) analyses are displayed above (below) the locations of the individual stations in (d).

al. (1969) and with the FGGE analyses (Lau, 1984) than the GFDL analyses.

The GFDL mean fields have overly smooth horizontal distributions and tend to underestimate zonal variations and features in the latitude band 40°–65°S. This is due to the sparse conventional rawinsonde network in the SH and the use of the zonal mean as the first guess in the GFDL analyses. The height and wind fields in the GFDL analyses are not in geostrophic balance in this region due to the sparsity of stations. The ASH analyses had much more data available over the SH oceans, mainly from satellite temperature soundings and from the interpretation of satellite imagery. All these suggest that most of the time-mean fields in

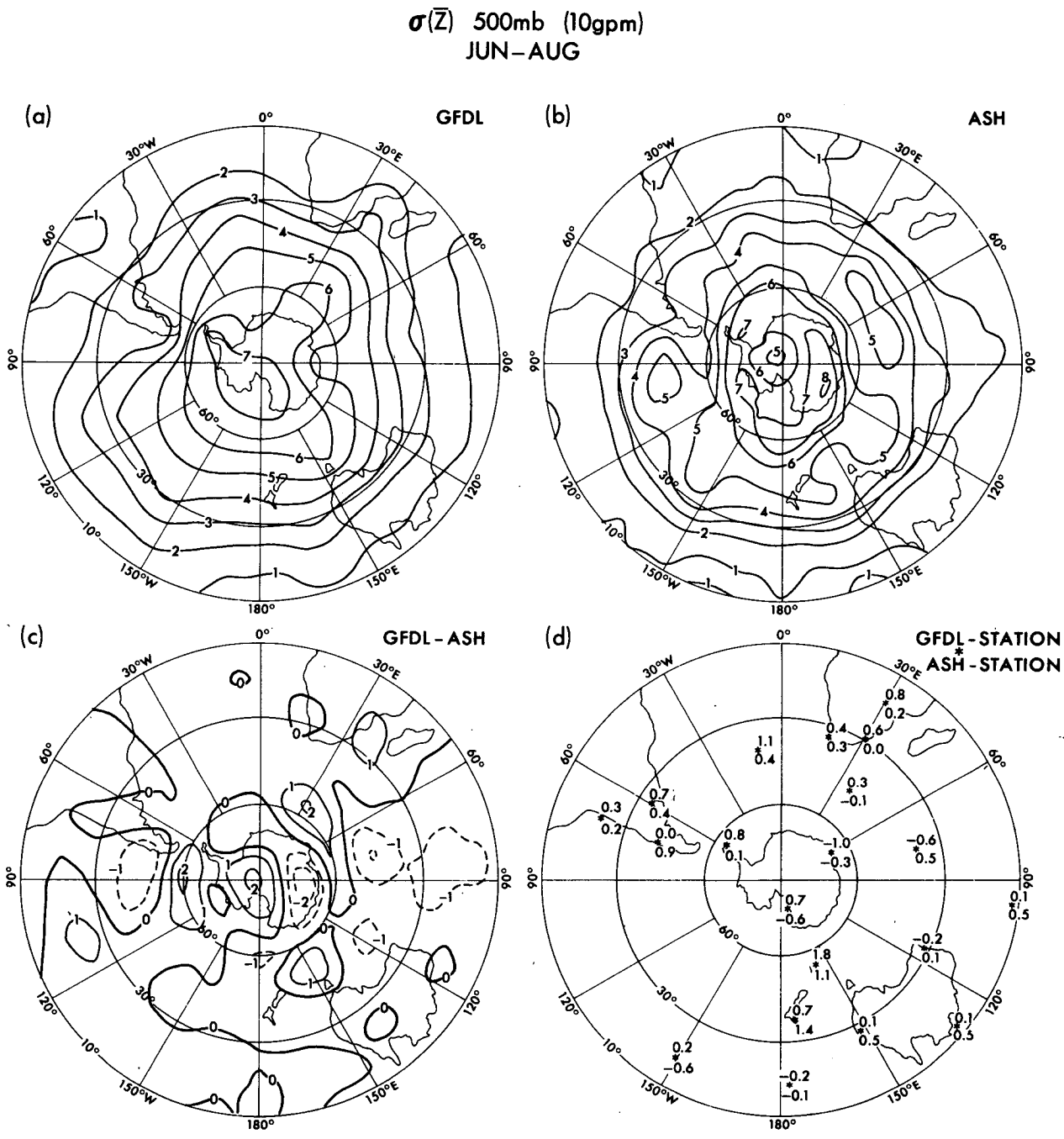

FIG. 20. As in Fig. 19 except for geopotential height (dam) at 500 mb.

the ASH analyses are closer to the "real" mean SH circulation. However, the ASH analyses are reliable only poleward of about 20°S because of the constraints in the operational analysis system.

An exception to this is that the mean temperature in the ASH analyses are unreliable at the 1000 mb level and, to a lesser extent, at the 850 mb level. This is due to a warm bias in the first-guess fields for the temperature analyses near the surface in the operational Australian analyses (Le Marshall et al., 1985). The GFDL mean temperature analyses in the lower troposphere are much better than the ASH analyses.

b. Daily transient eddy statistics

The differences of the transient eddy statistics between the two datasets are large near the surface and at the tropopause level, but are smaller in the middle

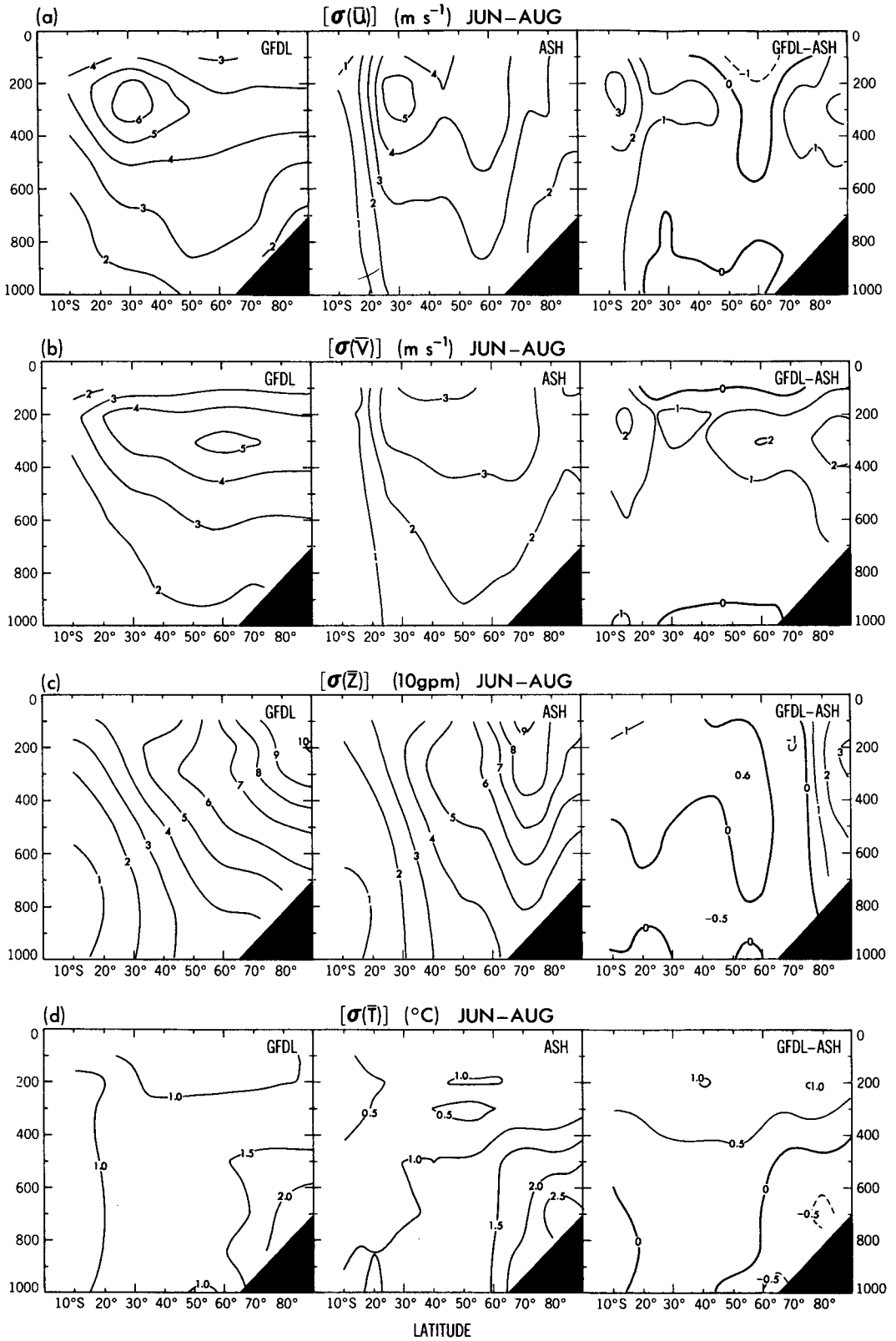

FIG. 21. Meridional cross sections of the winter zonal mean standard deviation of the monthly mean (a) zonal wind (m s^{-1}), (b) meridional wind (m s^{-1}), (c) geopotential height (dam) and (d) temperature (°C), based on GFDL analyses (left panel) and ASH analyses (middle panel). The differences between the corresponding fields from the two sets are shown in the right panel.

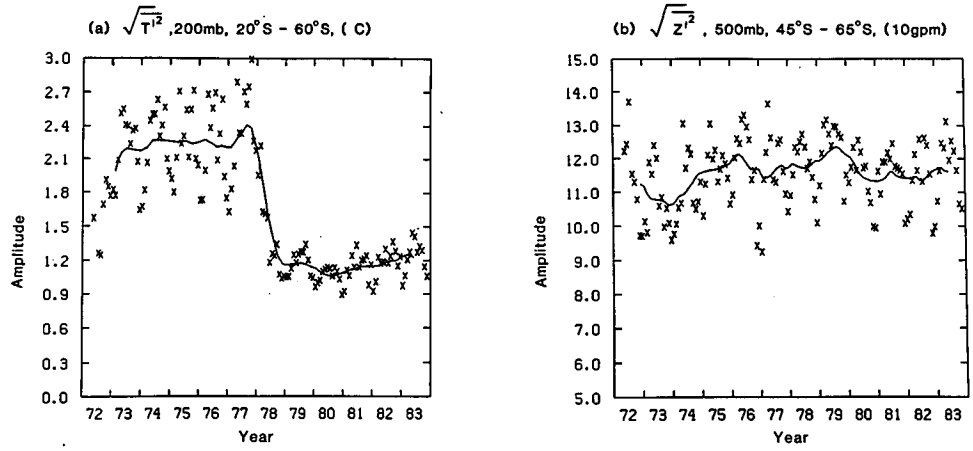

FIG. 22. Time series of the area-mean daily standard deviation of (a) temperature (°C) at 200 mb between 20° and 60°S and (b) geopotential height (dam) at 500 mb between 45° and 65°S. The crosses show the values for each month and the solid line is the 12-month running mean of the monthly values.

troposphere. The GFDL analyses have smoother horizontal distributions but generally larger amplitudes than the ASH analyses. The vertical distribution and amplitude of the zonal-mean transient eddy statistics from the GFDL analyses agree better with those for FGGE (Lau, 1984) near the surface and in the upper troposphere than the ASH analyses.

The horizontal distributions of these statistics in the ASH analyses are likely to be better in data-sparse regions than in the GFDL analyses because of the additional data sources available for the ASH analyses. However, it appears that the use of the zonal average for the first-guess fields in the GFDL analyses causes less problems for the transient eddy statistics than for the time-mean fields, because of the smaller zonal variations in the transient eddy statistics.

The largest differences between the two datasets appear to be due to deficiencies in the transient eddy statistics in the ASH analyses related with the constraints in the operational analysis system. These can be summarized as follows:

(i) The daily variability of the wind field at low latitudes (equatorward of 20°S) is underestimated at all levels because of the climatological constraint used in the operational Australian analysis procedure. This limits the daily departures of the wind at low latitudes from the climatological monthly mean wind of Taljaard et al. (1969).

(ii) The transient-eddy heat flux in the lower troposphere is underestimated due to the problems in the temperature analyses near the surface in the operational Australian analyses.

(iii) The ASH analyses underestimate the daily variability of temperature and wind in the upper troposphere, particularly at the tropopause level. This is due to the extrapolation technique used in the operational Australian analyses to give the first-guess field for thickness in the upper troposphere, which regresses towards the climatological thickness, and the use of satellite temperature soundings in the Australian operational database.

The coarse vertical resolution available in the satellite temperature soundings tends to smooth temperature fluctuations at the tropopause level. This can be seen clearly in Fig. 22, which shows a time series of the area-mean daily standard deviation of temperature at 200 mb between 20° and 60°S based on the ASH analyses. Satellite temperature soundings were included in the Australian operational database from 1976 on, leading to a marked reduction in the daily temperature variance in the upper troposphere, which was most apparent at the tropopause level.

The impact of the satellite temperature soundings is less important for the daily variability in geopotential height than for the temperature variability. The geopotential height variances in the upper troposphere are in good agreement when we compare the two datasets. Also, the satellite temperature soundings have had little effect on the ASH monthly mean fields in the upper troposphere, apart from providing an improved hemispheric data coverage.

Also shown in Fig. 22 is a time series of the area-mean daily standard deviation of geopotential height at 500 mb between 45° and 65°S from the ASH analyses. The interannual changes in this time series may be associated generally with changes in the database used in the operational Australian database: some initial problems with the analysis system in 1972, the inclusion of satellite temperature soundings since 1976 and the inclusion of surface pressure data from drifting buoys in 1979, associated with the Global Weather Experiment.

Since the interannual variations of the daily transient eddy statistics in the ASH analyses are mainly due to changes in the operational Australian database, no comparison has been made between the interannual

variability of the transient eddy statistics from the GFDL and ASH datasets.

To summarize these points about the transient eddy statistics, the zonal means from the GFDL analyses are better than those from the ASH analyses but the horizontal distributions from the GFDL analyses may be unreliable over data-sparse regions. In the middle troposphere (at the 700 and 500 mb levels), the differences of the zonal means are small and the horizontal distributions from the ASH analyses are likely to be more reliable.

c. Interannual variability statistics

The interannual variability statistics from the two datasets appear to agree better than for the mean fields or the transient eddy statistics, although there are still some large differences. It should be noted that there are likely to be large errors in estimating these interannual variability statistics using ten-year periods only, and that more reliable statistics would require much longer period datasets. It is likely that the horizontal distributions of these statistics are better in the ASH analyses over data-sparse regions due to the additional data available. However, the constraints in the operational Australian analyses may have led to deficiencies in some of the statistics, particularly at low latitudes and at the tropopause level.

Overall, the ASH dataset appears to be better for the mean fields (except for temperature in the lower troposphere) and for the variability statistics in the middle troposphere. The GFDL dataset is better for the mean temperature at low levels and the variability statistics for temperature near the surface or near the tropopause and for wind at low latitudes or near the tropopause.

These assessments of the reliability of the GFDL and ASH analyses of SH circulation statistics highlight the advantages and disadvantages of each dataset. They should enable a choice to be made of the most appropriate statistic from the two datasets for a range of purposes including the verification of atmospheric general circulation models, studies of the SH circulation and testing of numerical weather prediction models for the SH.

Acknowledgments. This study was carried out while the first author was a Visiting Scientist in the Atmospheric Analysis and Prediction Division at NCAR. He wishes to thank A. Kasahara and H. van Loon for making that visit possible. The data used in the Australian SH climatology was provided by the Australian Bureau of Meteorology. We are grateful to G. Kelly, N.-C. Lau, J. Le Marshall, R. Seaman, H. Savijärvi, K. Trenberth and H. van Loon for their comments on this study. We wish to thank A. Leicester for typing the manuscript and the Scientific Illustration Group at GFDL and J. Sheldon for preparing the figures.

REFERENCES

Cressman, G. P., 1959: An operational objective analysis system. *Mon. Wea. Rev.*, **87**, 367–374.

Karoly, D. J., 1985: An atmospheric climatology of the Southern Hemisphere based on ten years of daily numerical analyses (1972–82). II: Standing wave climatology. *Aust. Meteor. Mag.*, **33**, 105–116.

——, G. A. M. Kelly, J. F. Le Marshall and D. J. Pike, 1986: An atmospheric climatology of the Southern Hemisphere based on ten years of daily numerical analyses (1972–82). WMO Long-Range Forecasting Res. Rep. No. 7, WMO/TD No. 92, 73 pp.

Lau, N. C., 1984: A comparison of circulation statistics based on FGGE level III-b analyses produced by GFDL and ECMWF for the Special Observing Periods. NOAA Data Report ERL GFDL-6, 237 pp.

——, and A. H. Oort, 1981: A comparative study of observed Northern Hemisphere circulation statistics based on GFDL and NMC analyses. Part I: The time-mean fields. *Mon. Wea. Rev.*, **109**, 1380–1403.

——, and ——, 1982: A comparative study of observed Northern Hemisphere circulation statistics based on GFDL and NMC analyses. Part II: Transient eddy statistics and the energy cycle. *Mon. Wea. Rev.*, **110**, 889–906.

——, G. H. White and R. L. Jenne, 1981. Circulation statistics for the extratropical Northern Hemisphere based on NMC analyses. NCAR Tech. Note NCAR/TN-171+STR, 138 pp.

Le Marshall, J. F., G. A. M. Kelly and D. J. Karoly, 1985: An atmospheric climatology of the Southern Hemisphere based on ten years of daily numerical analyses (1972–82). I: Overview. *Aust. Meteor. Mag.*, **33**, 65–85.

Mo, K. C., and H. van Loon, 1984: Some aspects of the interannual variation of mean monthly sea level pressure on the Southern Hemisphere. *J. Geophys. Res.*, **89**, 9541–9546.

Newell, R. E., J. W. Kidson, D. G. Vincent and G. J. Boer, 1972 and 1974: *"The General Circulation of the Tropical Atmosphere and Interactions with Extratropical Latitudes", Vols. 1 and 2,* The MIT Press, 258 and 371 pp.

Obasi, G. O. P., 1963: Poleward flux of atmospheric angular momentum in the Southern Hemisphere. *J. Atmos. Sci.*, **20**, 516–528.

Oort, A. H., 1983: *Global Atmospheric Circulation Statistics, 1958–1973.* NOAA Prof. Paper 14, U.S. Govt. Printing Office, 108 pp.

——, and E. M. Rasmusson, 1971: *Atmospheric Circulation Statistics.* NOAA Prof. Paper 5, U.S. Govt. Printing Office.

Rosen, R. D., D. A. Salstein, J. P. Peixoto, A. H. Oort and N. C. Lau, 1985: Circulation statistics derived from level III-b and station-based analyses during FGGE. *Mon. Wea. Rev.*, **113**, 65–88.

Swanson, G. S., and K. E. Trenberth, 1981a: Trends in the Southern Hemisphere tropospheric circulation. *Mon. Wea. Rev.*, **109**, 1879–1889.

——, and ——, 1981b: Interannual variability in the Southern Hemisphere troposphere. *Mon. Wea. Rev.*, **109**, 1890–1897.

Taljaard, J. J., H. van Loon, H. L. Crutcher and R. L. Jenne, 1969: *Climate of the Upper Air: Southern Hemisphere,* Vol. 1 NAVAIR 50-IC-55, Chief of Naval Ops., 135 pp. [Available from Naval Weather Services Command, Washington, DC 20390]

Trenberth, K. E., 1979: Interannual variability of the 500-mb zonal mean flow in the Southern Hemisphere. *Mon. Wea. Rev.*, **107**, 1515–1524.

——, 1981: Observed Southern Hemisphere eddy statistics at 500 mb: frequency and spatial dependence. *J. Atmos. Sci.*, **38**, 2585–2605.

——, 1982: Seasonality in Southern Hemisphere eddy statistics at 500 mb. *J. Atmos. Sci.*, **39**, 2507–2520.

——, 1984: Interannual variability of the Southern Hemisphere circulation: representativeness of the year of the Global Weather Experiment. *Mon. Wea. Rev.*, **112**, 108–125.

van Loon, H., 1980: Transfer of sensible heat by transient eddies in the atmosphere of the Southern Hemisphere: an appraisal of the data before and during FGGE. *Mon. Wea. Rev.*, **108**, 1774–1781.

——, J. J. Taljaard, R. L. Jenne and H. L. Crutcher, 1971: *Climate of the Upper Air: Southern Hemisphere,* Vol. 2, NAVAIR 50-IC-56, Chief of Naval Ops., 42 pp. [Available from Naval Weather Services Command, Washington, DC 20390]